Fermilab Test Beam Facility Annual Report: FY19

M. Rominsky[1], E. Schmidt[1], E. Niner[1], L. Uplegger[1], R. Rivera[1], E. Angelico[2], B. Adams[2,3], F. Clark[2], A. Elagin[2], H. Frisch[2], M. Popecki[2,3], E. Spieglan[2], A. Sousa[4], M. Wallbank[4], M. Sergeeva[5], D. Neff[5], B. Chan[5], O. Tsai[5], A. Kisilev[6], T. Lin[7], D. Chen[8], D. Kapukchyan[8], Y. Goto[9], Y. Miyachi[10], G. Nukazava[10], R. Ehrlich[11], S. Boi[11], Koji Nakamura[12], Shun Ono[12], Miho Yamada[12], Toru Tsuboyama[12], Kazuhiko Hara[13], T. Anderson[11], M. Arenton[11], P. Barria[11], A. Benaglia[14], O. Cerri[15], B. Cox[11], I. Dutta[15], M. Hermann[16], M. Joyce[11], G. Karaman[14], G. Kopp[17], N. Lu[15], M. Lucchini[17], J. Mao[15], A. Mohammadi[18], L. Paredes[15], C. Pena[15], C. Rude[16], B. Tannenwald[11], C. Wang[15], S. White[11], S. Xie[15], S. Aune[19], B. Azmoun[6], W. Fan[20], A. Kiselev[6], I. Mandjavidze[19], C. Perez-Lara[20], M. Purschke[6], M. Revolle[19], M. Vandenbroucke[19], C. Woody[6], C. Dean[21], M. Durham[21], H. van Hecke[21], G.J. Kunde[21], X. He[22], J. Huang[6], X. Li[21], Z. Li[21], S. Lim[23], M.X. Liu[21], Y.C. Morales[21], C. O'Shaughnessy[21], M.L. Purschke[6], A. Raymer[21], C. da Silva[21], W. Sondheim[21], X. Sun[22], M. Taylor[24], A. Tkatchev[21], S. Uemura[21], M. Chiu[6], E. May[25], S. Nelson[26], C. Scarlett[26], J. Xie[25], T.K. Hemmick[2]0, K. Delmelt[2]0, T. Sakaguchi[6], J. Huang[6], J. Freeman[1], D. Lincoln[1], S. Uzunyan[27], S. Blusk[28], J. Wang[28], S. Ely[28], K. Kim[28], Z. Li[28], M.Wilkinson[28], D. Nguyen[2]9, G. Hanson[3]0, A. Frankenthal[31], J. Thom[31], A. Hassani[23], S. Wagner[23], S. Dittmer[32], C. Mills[32], T. Roy[32], J. Yoo[32], C. Suarez[33], J. Castaneda[34], B. Bentele[35], B. Bylsma[35], B. Cardwell[35], C. Hill[35], R. Gonzalez[36], A. Guerrero[36], S. Norberg[36], J. Thieman[37], M. Jones[37], T. Cheng[38], H. Acharya[39], L. Moore[39], S. Spanier[39], Y. Akiba[9,40], K. Cheng[41,40], E.Desmond[6], T. Hatchiya[5,40], J. Haggerty[6], S. Hasegawa[43,9], T. Kondo[44,9], C. Kuo[41], I. Nakagawa[9,40], R. Nouicer[6], C. Shih[41,40], A.i[42,9], T. Todoroki[40], R. Xiao[37,40], W. Xie[37], M Murray[45], M Nickels[45], Q Wang[45], R Longo[46], C Lantz[46], T Zhang[46], Y Kulinich[46], S Yang[46], Sean Preins[46], A Mankolli[46], J Bryant[46], R Karanam[47], Z Citron[47], E Adams[48], J. Metcalfe[25], M. Benoit[49], V. Bhopatkar[25], W. Islam[50], M. Jadhav[25], J. Lambert[51], J. Muse[51], S. Nagasamudram[2], S. Shrestha[2], D. Wilbern[51], W. Wu[2], J. Xie[25], L. Xu[6], A. Apresyan[1], C. Rogan[45], M. Obertino[52], R. Heller[1], S. Xie[15], C. Pena[1], N. Minafra[45], A. Ovcharova[53], M. Hussain[2], T. Wamorkar[54], F. Siviero[52], T. Isodori[45], M. Lazarovitz[45], A. Abreu[45], A. Koziol[55], D. McGraw[45]

November 14, 2019

[1]Fermi National Accelerator Laboratory
[2]University of Chicago
[3]Incom Inc.
[4]University of Cincinatti
[5]University of California Los Angeles
[6]Brookhaven National Laboratory
[7]Texas A&M University
[8]University of California Riverside
[9]RIKEN (Japan)
[10]Yamagata University (Japan)
[11]University of Virginia
[12]High Energy Accelerator Research Organization (KEK)
[13]University of Tsukuba
[14]INFN-Milano
[15]California Institute of Technology
[16]University of Iowa
[17]Princeton University
[18]Kansas State University
[19]CEA Saclay
[20]Stony Brook University
[21]Los Alamos National Laboratory
[22]Georgia State University
[23]University of Colorado
[24]Massachusetts Institute of Technology
[25]Argonne National Laboratory
[26]Florida A&M University
[27]Northern Illinois University
[28]Syracuse University
[29]University at Buffalo
[30]University of California at Riverside
[31]Cornell University
[32]University of Illinois at Chicago
[33]Johns Hopkins University
[34]University of Nebraska at Lincoln
[35]The Ohio State University
[36]University of Puerto Rico at Mayaguez
[37]Purdue University
[38]Purdue University Northwest
[39]Univerity of Tennessee at Knoxville
[40]RIKEN-BNL Research Center
[41]National Central University

[42]Nara Women's University
[43]Japan Atomic Energy Agency
[44]Tokyo Metropolitan Industrial Technology Research Institute
[45]University of Kansas
[46]University of Illinois, Urbana Champaign
[47]Ben-Gurion University
[48]University of Maryland
[49]Université de Genève
[50]Oklahoma State University
[51]University of Oklahoma
[52]Torino
[53]University of California Santa Barbara
[54]Northeastern
[55]AGH University of Science and Technology, Krakow

Abstract

This Technical Memorandum (TM) summarizes the Fermilab Test Beam Faciltiy (FTBF) operations for FY2019. It is one of a series of annual publications intended to gather information in one place. This TM discusses the experiments performed at the Test Beam from November 2018 to July 2019. The experiments are listed in Table 1. Each experiment wrote a summary that was edited for clarity and is included in this report.

1 Summary of FY19

The Fermilab Test Beam Facility continues to be an important resource for experiments and for detector R&D. In FY19, we supported a very heavy load of users, primarily from the collider physics community. Beam was dominated by user requests, with only a few days dedicated to facility studies and improvements. Highlights from the FY19 year include:

- Hosting summer interns. One CCI, two SIST, and one TARGET intern worked primarily on expanding otsDAQ .
- Both MCenter and MTest were utilized during the full year.
- In MCenter a new teriary beamline in MC7b was established for the NOvA test beam.
- *otsdaq* commissioning with the wire chambers and Cherenkov telescope. otsDAQ monitoring tied into ACNET to feed parameters back to operators.
- We purchased new low and high voltage Weiner MPods.

- Work began to modernize and expand slow controls for the gas shed.
- Updates and formalization of facility policies and procedures for user groups. Overhaul of the facility website and documentation in progress.
- A paper is in progress on facility capabilities. Planning beam studies in winter 2020 to gather additional data.

During FY19, we hosted 21 experiments (Table **??**) from all areas of physics. This year was busy at the test beam. Out of the thirty beam weeks of running, 55 user weeks took place. Often multiple groups ran in MTest at the same time. The facility was fully utilized other then reduced requests over the holiday period. In May and June of 2019 the accelerator operations budget forced reduced running conditions with five days on followed by nine days off. This schedule lost 36 days of potential beam and effected the run plans of ten groups. These groups adjusted schedules and ran as many as five at a time to maximize the available beam. These groups worked well together and made efficient use of the available beam, all groups were able to achieve some results. The 6.1a telescope received heavy use from LHC groups throughout the year. With the long CERN shutdown we saw additional new users at FTBF. In MCenter significant construction took place throughout FY19 to establish a new tertiary beamline and construct the NOvA detector. Commissioning data was taken in the last month of beam and the physics run will commence in FY20.

Throughout the year, we worked on the data acquisition system for the test beam and had some success. The *otsdaq* platform was used extensively to read out the facilty wire chambers and beam profile monitoring code was ported from offline into the DAQ system. These monitoring tools were connected to ACNET and in FY20 we plan to interface with the MCR so they are able to see the same information experimental groups are looking at. Work was done with the Cherenkov detector to integrate the frontend and the facility NIM and CAMAC crates were mapped and audited. Work began over the summer on an otsDAQ interface to readily make facitily intrumentation data from the system availabe externally to user DAQs through a shared memory segment and is in final testing.

The Accelerator delivered over 120,00 pulses to the test beam, as seen in Figure 1. We are grateful to the accelerator for the beam they delivered to us.

2 Iradiation Test Facility

Many users at FTBF bring irradiated sensors/chips/devices to study in the beam or schedule time at FTBF before and after an irradiaiton run to measure effects. There is strong support from the HL-LHC upgrade groups, sPHENIX and the HEP community for a proton irradiation facilty at Fermilab.

An irradiation facility is under construction at Fermilab in the MuCool Test Area (MTA) located just downstream of the linac. During FY19 cleanup, efforts took place

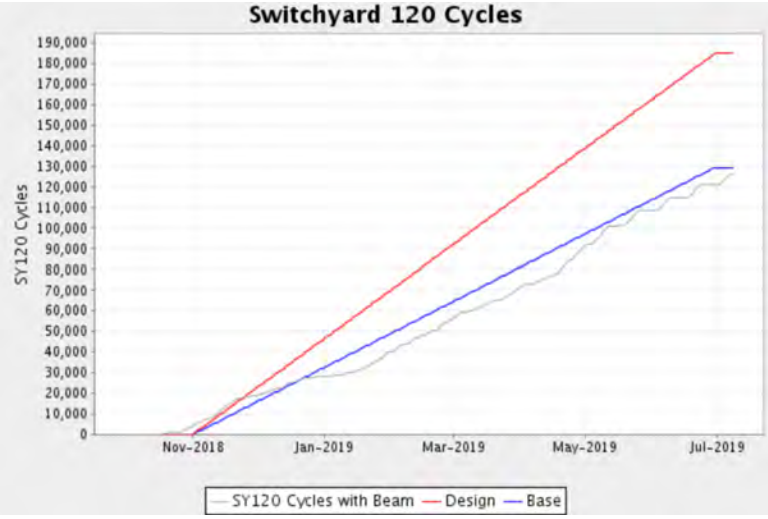

Figure 1: Delivery of pulses to the test beam. Note that this includes data sent to both MCenter and MTest. The flat regions represent change overs or problems in the beam. Note the step features in May and June 2019 from the 5 day on, 9 day off running conditions.

to remove existing equipment in MTA. Funding has been received for FY20 to build the beamline and irradiation cave and construction and shielding assessments are underway. Nominally construction will wrap up in January 2020 and after a commissioning period have beam available to users in March for the last three months of the acclerator run before the summer shutdown.

The irradiation area will receive 400 MeV protons from the linac during the slow spill extraction, causing no additional overhead on the Fermilab program. During this initial run period only silicon will be irradiated and devices will not be powered or cooled in order to reduce the combinatorics of the shielding assessment and construction times. During the 2020 summer shutdown additional infrastructure will be added and the shielding assessment expanded. To allow setup, irradiation, and cool-down there will be one user per week. Scheduling of time in the facility will be handled through FTBF since the majority of users will use both facilities in a coordinated fashion.

3 Research Overview at the Test Beam

In FY19, we saw user groups from LHC and non-LHC collider physics, neutrinos, muons, and general R&D. Many LHC groups frequented the facility, often testing irradiated samples. In FY19 sPHENIX achieved PD-2/3 and noted FTBF played a significant role in passing the review. We saw three new experimental efforts in MTest and a NOvA assembled a detector and tertiary beamline in the MC7b area. The individual reports in the

next section fully describe the tests that were carried out.

3.1 Publications

The groups at the test beam will often report their findings in internal notes, at conferences, and in published journals. This past year, all 21 groups have plans for publications or have presented results at conferences. Graduate student Tanvi Wamorkar from Northeastern University won second place in the APS DPF poster competition for work with the T1409 endcap timing layer. This year, there was one article published in a journal, with several in preparation. There were three PhD theses completed on work based on the LArIAT experiment.

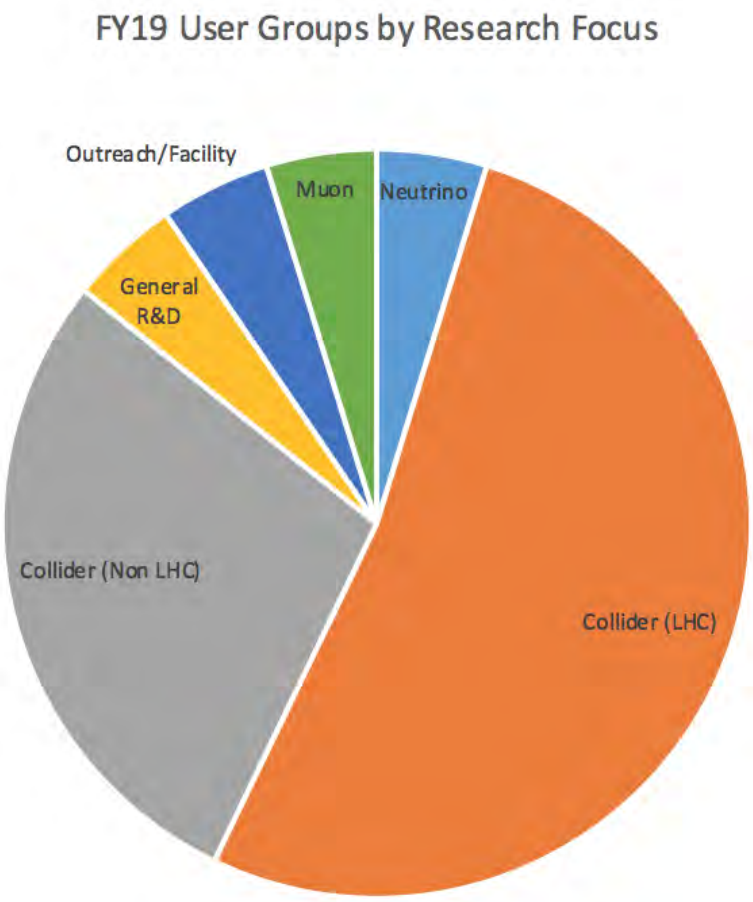

Figure 2: Breakdown of FY19 users by research focus. This year, we had a large group of collider experiments.

Experiment Number	Description
T-992	INFN CMS Pixels Phase II Sensors
T-992	US CMS Pixels Phase II Sensors
T-992	RD53a Chip Tests
T-992	CMS Outer Tracker Phase 2
T-1018	Tungsten powder calorimeter
T-1043	Mu2e CRV scintillation counters
T-1068	Beam Tests of the SVX4 Telescope
T-1224	ATLAS Pixel Telescope Tests
T-1409	CMS Timing Barrel
T-1409	CMS Timing Endcap
T-1429	Performance Study of a planar GEM and MM detector with zigzag pad readout
T-1439	sPHENIX Silicon Strip Tracker (INTT) Testsu
T-1441	sPHENIX MAPS Vertex Detector (MVTX)
T-1450	EIC PID R&D: Argonne MCP-PMT Test
T-1473	FLYSUB-Consortium Tracking and RICH Performance Evaluation
T-1512	NOvA Test Beam
T-1516	CMS HGG-BH Tests
T-1557	Seed germination for ACT-SO student
T-1564	LHCb Upstream tracker
T-1575	Joint Zero Degree Calorimeter Project
ORC-1553	LAPPD-TOF phase 0

Table 1: Test Beam experiments performed in FY19.

FTBF FY19 By the Numbers	
Professional Class	*Total*
Postdoc	40
Scientist/Faculty	81
Graduate Student	88
Engineers/Techs	8
Undergraduate students	19
Total	236
Experiment Focus (TSWs)	*Total*
Neutrino	4
Collider (LHC)	36
Collider (Non-LHC)	11
Muon	2
General R&D	1
Outreach/Facility	1
Publications	*total*
Journals	1
Conference presentations	Many groups
Posters	Many groups
Internal Notes	Information coming
Theses	3

Table 2: Statistics for Test Beam experiments performed in FY19. Note that the Experiment focus is listed in weeks of beam taken by the group.

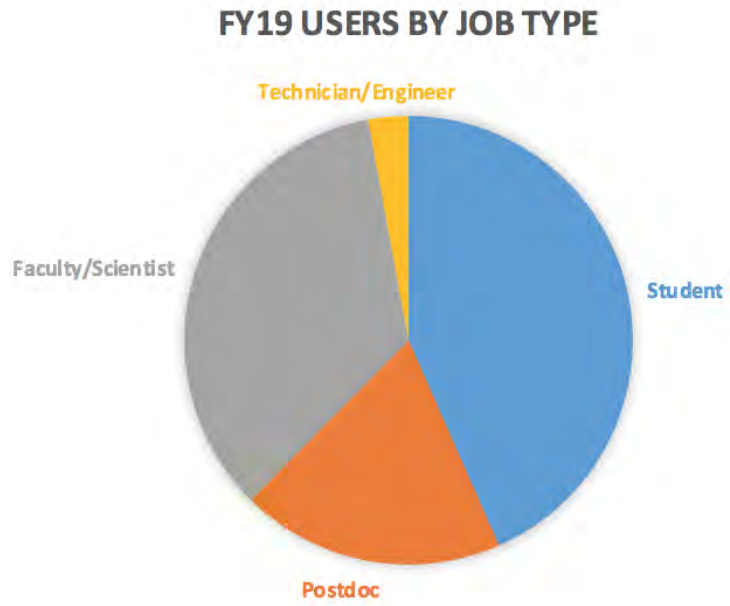

Figure 3: Breakdown of FY19 users by professional class.

4 T-992 Tests of radiation-hard sensors for the HL-LHC

L. Uplegger[1], R. Rivera[1]

[1]Fermilab

Beam Used: 120 GeV Protons
Run Dates: Nov 6-Nov 20, Nov 27-Dec 17 2018, Feb 6- Mar 20, Jun 3-June 8 2019

Motivation and Goals

At the HL-LHC, after 2500 pb^{-1} of data, the Expected maximum fluence for the pixel region ($\sim$ 3 cm) will be $2.5 \times 10^{16} n_{eq}/cm^2$. To cope with this unprecedented radiation environment, there have been quite a few international collaborations formed to find possible solutions for vertex and tracking detectors at the HL-LHC. These include the RD42, RD49, and RD50 collaborations. A variety of solutions have been pursued. These include diamond sensors, 3D sensors, MCZ planar silicon detectors made from MCZ wafers, epitaxial, p-type silicon wafers and thin silicon detectors. The experimenters wish to compare the performance of this wide variety of detectors in a test beam before and after irradiation. To do so, the experimenters use the FTBF pixel and strip tracking telescopes which have

$\sim$ 6 m resolution at the device under test. In particular, the experimenters are planning to study the charge collection efficiency of irradiated and un-irradiated devices and the spatial resolution as a function of the applied sensor voltage bias and the track incident angle.

For the foreseen upgrade in luminosity CMS will also upgrade the strip tracker and the new Read Out Chip (ROC) need to be tested in more realistic conditions than on a test bench. Strip-Strip sensors configuration has been tested to study detector efficiency and time walk.

Setup

The pixel and strip telescopes, shown in Figure 4 are read out through a custom DAQ system known as CAPTAN. A gigabit Ethernet board is used to route the data to a computer which is connected to a Fermilab server. The readout boards are located close to the detector in the hut, and share a common clock and trigger signal. The detectors themselves may be operated up to $\sim$ 800 V.

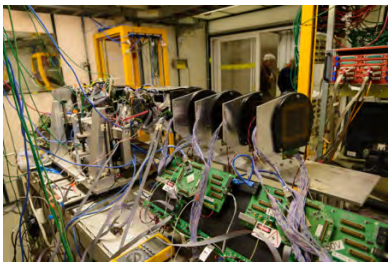

Figure 4: In situ T-992 test beam setup.

Results and Publications

The experimenters studied 3D silicon, a new prototype of planar sensors with a small pitch (25μm) and several n-on-p type silicon thin planar sensors. 3D tracking detectors and thin n-on-p sensors are promising radiation-hard candidates to replace planar n-on-n detectors in the HL-LHC. Radiation damage effects are measured with regards to charge collection, efficiency, and resolution of the particle tracks in beam tests, as well as leakage current and pixel noise. We have studied one variety of 3D sensors: 1E, i.e. with just one junction column, irradiated at CERN up to a fluence of $1 \times 10^{16} \mathrm{n_{eq}/cm^2}$.

The 3D devices are fabricated at the Fondazione Bruno Kessler (FBK) in Italy, while thin n-on-p sensors are fabricated at FBK and HPK. These new devices have all patterns with pitches of 25x100 or 50x50 $\mu\mathrm{cm}^2$. Different designs, mostly with or without punch-through, and with bump pads on top or aside the junction columns, were tested to compare

their performance before and after irradiation to converge to the most efficient and radiation hard fabrication process. These combined efforts from the European, testing devices from FBK, and US collaborators, testing devices from FBK, is narrowing down the possible candidates for the upgrade and is also converging on the final design that will then be mounted on the new read out chip coming from the RD53 collaboration.

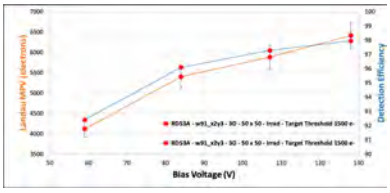

Figure 5: Landau Most Probable Value (MPV) and hit collection efficiency as a function of the bias voltage for irradiated 3D sensors up to $1 \times 10^{16} \mathrm{n_{eq}/cm^2}$.

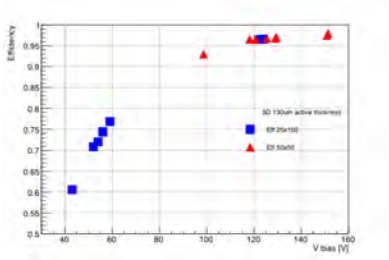

Figure 6: Hit detection efficiency as a function of the bias voltage for irradiated 3D sensor up to $1 \times 10^{16} \mathrm{n_{eq}/cm^2}$.

The collaboration is also testing devices for the CMS Outer Tracker phase II upgrade and in December 2018 a new prototype of strip-strip (2S) module was tested after undergoing 2 irradiation cycles for a total integrated dose of $4.4 \times 10^{14} \mathrm{n_{eq}/cm^2}$. The module was the first prototype with the new and almost final design of the read-out chip called CBC3. In December of the previous year we measured efficiency, charge collection, time walk and assessed the overall properties of the un-irradiated chip which worked as expected. In May 2018 instead, we assessed the performance after a total dose of $2 \times 10^{14} \mathrm{n_{eq}/cm^2}$. In December 2018 instead the module was re-tested to check the overall performances to a dose that is above the maximum expected in HL-LHC. The module performed very well before and after irradiation increasing the confidence in the collaboration to have already a reliable and working candidate for the upgrade.

5 T-992 U.S. CMS Pixels Phase II Sensors

Collaborators

University at Buffalo Duong Nguyen*

University of California at Riverside Gail Hanson*

Cornell University Andre Sterenberg Frankenthal*, Julia Thom

University of Colorado at Boulder Abbas Hassani, Stephen Wagner*

University of Illinois at Chicago Susan Dittmer*, Corrinne Mills*, Titas Roy*, Jieun Yoo*

Johns Hopkins University Cristina Mantilla Suarez,

University of Nebraska at Lincoln Joaquin Siado Castaneda*

The Ohio State University Benjamin Bentele, Benjamin Bylsma, Bryan Cardwell*, Chris Hill

University of Puerto Rico at Mayaguez Ricardo Gonzalez*, Alvaro Guerrero*, Scarlet Norberg*,

Purdue University Jason Thieman*, Matthew Jones

Purdue University Northwest Tongguang Cheng*

Univerity of Tennessee at Knoxville Himal Acharya*, Luke Moore*, Stefan Spanier*,

All names and institutions are in alphabetical order. Asterisk indicates physical presence at FBTF, i.e. anyone who took a shift or supervised on-site (i.e. faculty). Other names include people who are analyzing data or made other technical contributions, such as dedicated circuit-board development for the interface between the devices and our DAQ. Fermilab staff scientiest Lorenzo Uplegger provided significant effort for the analysis and software development. We also benefitted from close collaboration with the INFN Firenze and Milano Bicocca groups, who let us use their cold boxes to keep the irradidated devices cold and dry, and also provided guidance on analysis.

Beam Used: 120 GeV Protons
Run Dates: Nov 6-Nov 20, Feb 6- Feb 19, Jun 3-June 8, Jun 17 - Jun 22 2019

Motivation and Goals

The CMS pixel detector upgrade for the HL-LHC must withstand unprecedented radiation fluence, up to 2×10^{16} neutron-equivalent per cm^2 over the lifetime of the detector. To deliver the precision tracking needed to discriminate the 200 interactions per bunch crossing while withstanding the radiation dose, improvements to both the sensors and readout chips (ROCs) are needed. The first prototype of the ROC, the RD53A chip, has been available for testing starting in April-May 2018. We commissioned its interface with the FTBF beam telescope in June-July 2018.

Our primary goal for this past year was to test the radiation hardness of the proposed pixel sensors and ROCs at fluences realistic for the innermost pixel layers during the lifetime of the HL-LHC. In November we tested sensor-ROC assemblies which had not been irradiated to establish a baseline. All of them used the RD53A prototype ROC, but with different pixel shapes and biasing schemes for the sensors. The devices were irradiated to half or all of the expected fluence using a beam of 800 MeV protons at the LANSCE facility at Los Alamos National Laboratory. At FTBF, using reference tracks from the beam telescope, we planned to measure efficiency and charge collection as a function of the bias voltage, and hit resolution as a function of incidence angle. European irradiation facilities cannot at present provide as much fluence at a reasonable radiation dose[1], so we are in a unique position to give input on the need to replace the innermost layer of the pixel detector partway through the HL-LHC.

The variety of institutions participating, many with just one or two people, indicates the breadth of support from the LHC Physics Center (LPC), a CMS organization hosted by Fermilab. It also represents recognition that test-beam work is a unique opportunity for students and postdocs. Unlike the years-long timescale and 3000-person effort of CMS as a whole, we plug in the detectors, calibrate them, define data quality criteria, debug problems, monitor data-taking, and finally analyze the data within the space of a few weeks. Our effort has, as a result, had a secondary benefit of training young scientists in hardware and operations including real-time problem solving.

Setup

Our RD53A sensor+ROC devices were set up in Area 6.1a of FBTF with the silicon-strip and pixel telescope, as shown in Fig. 7. The OTSDAQ software was used to read out the

[1] lower-momentum protons produce a higher dose rate, resulting in more damage to the readout electronics and more material activation.

Figure 7: Arrangement of the DUT (in coldbox) and the strip and pixel telescopes in the beamline, as used for the February 2019 run.

telecope data, configure our device, and start and stop runs. We used the 120 GeV proton beam.

The devices under test (DUTs) were mounted in an insulated box ("coldbox") with dry air (nitrogen) from the facility and cooling lines with a water and proplyene glycol mix circulating through a chiller. Inside the coldbox, the device is mounted so that the ROC is in thermal contact with a heat sink and Peltier to transfer heat from the ROC to the chiller water. The device was read out using the "YARR" software from a standalone PC in the enclosure. The PC had an FPGA board (an XPressK7) mounted in the PCIe slot on the motherboard, with daughter cards designed by the OSU team to connect to the DUT and bring in the external trigger signal from the scintillator in the telescope.

Analysis has been done using the Monicelli and Chewie software suites developed by FNAL and INFN groups. Monicelli reconstructs hit clusters and tracks, and has tools for the alignment of the DUT and telescope planes. Chewie analyses the resulting tracks and hits, producing measurements of the efficiency, resolution, and cluster charge.

Results and Publications

Due to unanticipated problems with the radiation hardness of the silicone used to encapsulate the wirebonds, we could only establish communication with two of the devices. One had only intermittent communication and could not be tuned to low thresholds, even cold. The other could be operated reliably and tuned down to a 1400 electron threshold. It is the device used for all results presented here. The pixel size is 50×50 μm^2, the thickness of the sensor is 150 μm, and the doping type is n-in-p.

The leakage current was measured at different bias voltages and temperatures. It exhibits the expected strong dependence on temperature. There is a suggested current limit of 500 μA to the full device to avoid damage to the ROC. The temperature and current limit combined set the maximum operating bias voltage, but heavily radiation-damaged sensors require large ($>$ 100V) biases to produce a sufficient depletion region for charged particle detection. Figure 8 (left) shows the measured leakage current as a function of bias voltage and temperature. At -30C, with the chiller and coldbox Peltier at their operational limits, we could reach the maximum suggested bias voltage for the device, -800 V.

The device was tuned to different thresholds, and 1400 electrons was the lowest threshold obtained. For simplicity, only the "linear" front-end was used for most runs, which also corresponds to the analog front-end design that CMS will use to build the final pixel detector. We measured the efficiency, defined as the fraction of reconstructed telescope tracks for which a hit is found in the DUT nearby the point where the track crosses the plane of the DUT. Figure 8 (right) shows the measured efficiency as a function of bias voltage for different operating points of temperature and threshold. The efficiency increases with bias voltage, corresponding to an increase in the depth of the depletion region, and decreases as the threshold is increased. At -30C, -800V, and a threshold of 1400 electrons, we achieve an efficiency of over 90%.

We also calibrated the gain of the ROC+sensor using an internal charge injection circuit. This determines, for each pixel, the conversion of the ADC output, a 4-bit measurement of time over threshold, to a number of electrons. Figure 9 shows the distribution of the calibrated measured cluster charge for two bias voltages at the same threshold (1400e) and temperature (-30C). The most probable value is higher for the larger bias voltage, supporting the hypothesis that increasing the bias voltage increases the depletion region.

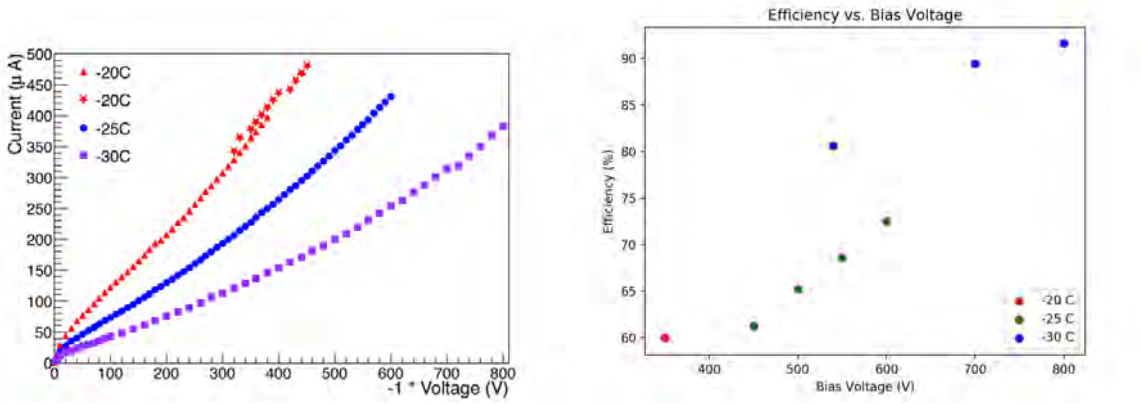

Figure 8: Left: Current as a function of bias voltage for the device under test, at different temperatures. Right: Hit-finding efficiency as a function of bias voltage at different operating points. Green points are with a threshold of 3000 electrons, blue points are at 1400 electrons, and red points at 1500 electrons.

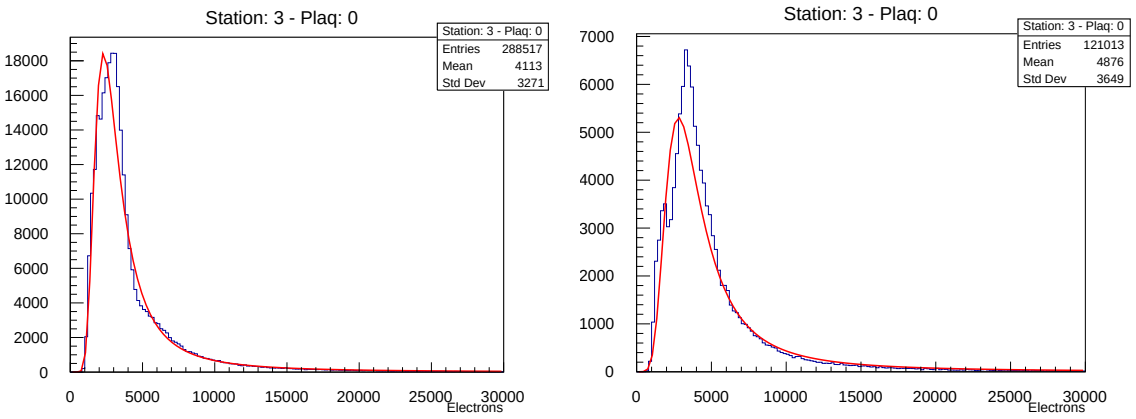

Figure 9: Distribution of measured charge using a threshold of 1400 electrons and a bias voltage of -540V (left) and -800V (right). The most probable value is 2400 electrons for -540V and 3000 electrons for -800V.

6 T-1018 Tungsten Powder Calorimeter

M. Sergeeva[1], D. Neff[1], B. Chan[1], O. Tsai[1], A. Kisilev[2], T. Lin[3], D. Chen[4], D. Kapukchyan[4], Y. Goto[5], Y. Miyachi[6], G. Nukazava[6]

[1]University of California Los Angeles
[2]Brookhaven National Laboratory
[3]Texas A&M University
[4]University of California Riverside
[5]RIKEN (Japan)
[6]Yamagata University (Japan)

Beam Used: 4 GeV - 70 GeV pion mode, 120 GeV protons, 30 GeV muon mode
Run Dates: April 3 - April 24, 2019

Motivation and Goals

We are continuing development of different technologies for sampling calorimeters for upgrades of experiments at RHIC (STAR Forward Calorimeter System (FCS), sPHENIX) and future Electron Ion Collider. This was fifth test run for eRD1 (EIC Calorimeter Consortium) following successful test runs in 2012, 2014, 2015, and 2016. The main goal this time was to calibrate FCS for STAR forward upgrade (EM+HAD), and to investigate dual readout method for hadronic calorimeters using timing utilizing same detector with different DAQ and readout sensors.

Setup

We used the MT6.2-B area for the experimental setup. Instrumentation provided by the test beam facility included a Lead Glass calorimeter, movable table 2B, alignment laser system, Cerenkov counter, CAMAC and NIM crates, some signal cables, patch panels, cameras. In addition we used the MWPC tracking system as a stand-alone system for monitoring beam conditions. The calorimeter is shown in Figure 10

Results and Publications

The energy resolution for electrons and hadrons (shown for two different light collection schemes) both meet STAR FCS requirements. With that, successful R&D phase for FCS is finished. FCS is presently under construction (funded by NSF) with targeted date of data taking at RHIC in Run 2022. Test runs in 2014 and 2019 were extremely useful to bring FCS project to construction stage. The exploratory dual readout test for EIC R&D

Figure 10: Experiment setup.

with FCS, which was not optimized for such purposes, shows that with Fe/Sc composition it is little hope to improve energy resolution using timing method. However, MC studies performed after the test run suggested that with Pb/Sc structure we may get better result, which is of great interest for EIC. We are planning to continue these studies with probable short test run at FNAL in spring 2020. Test Run 2019 was the first test run for members of recently formed UC EIC Consortium. It provided great opportunity for students from UC system to participate in EIC calorimeter R&D program. We are anticipating that UC EIC Consortium will continue to use FANL test beam facility to develop calorimeters for EIC in near future.

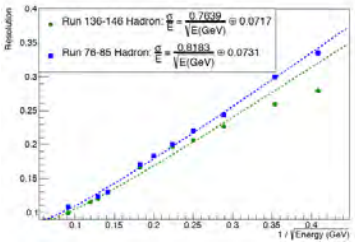

Figure 11

7 T-1043 Mu2e CRV Scintillation Counters

R. Ehrlich[1], S. Boi[1]

[1]University of Virginia

Beam Used: 120 GeV Protons
Run Dates: October 24 - November 6, 2018

Motivation and Goals

Several configurations of prototype scintillation counters for the Mu2e Cosmic Ray Veto (CRV) detector were tested. The 3 m long counters were made of extruded plastic scintillator and contained 2 WLS fibers (1.4 mm diameter) readout by 2 mm x 2 mm SiPMs on both ends. Two counters are glued together to form a discounter.

Goals:

- Measure the photoelectron (PE) yield at various locations at the CRV dicounters (longitudinal and transverse scans) to verify that the required PE yield can be achieved.
- Measure PE yields of older counters which were already measured in 2016 and 2017 to estimate the aging of the counters.
- Test new CMBs.
- Bias scan of the SiPMs.

Setup

Dicounters were tested up to 7 at a time as shown in Figure 12. Front End Board (FEB) readout electronics were mounted above the dicounters and data was sent to the control room through ethernet connections. XY scans were done by remote operation of the movable table and the mounting frame could be manually tilted for angular scans.

Results and Publications

Figure 13 shows the PE yield distribution for a proton beam which was directed at a CRV counter 1 m away from the readout. The most probable PE value of both SiPMs (of one side of a counter) combined is 103.8 PEs. This exceeds the required PE yield. Publication of the full test beam results is pending.

Figure 12: Photo of T-1043 setup showing CRV dicounters mounted on the movable table.

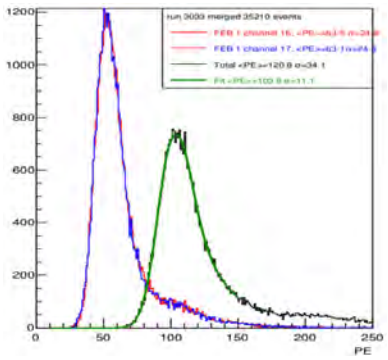

Figure 13: PE distributions for protons hitting a CRV counter 1 m away from the SIPMs. (red, blue) PE distributions for each of the two SiPMs, (black) combined PE distribution, (green) Gauss+Landau fit of the combined PE distribution

8 T-1068

Koji Nakamura[1], Shun Ono[1], Miho Yamada[1], Toru Tsuboyama[1], Kazuhiko Hara[2]

[1]High Energy Accelerator Research Organization (KEK)
[2]University of Tsukuba

Beam Used: 120 GeV Protons
Run Dates: February 20 - March 5, 2019

Motivation and Goals

The following three devices are tested at the beam test in FY19. 1) A planar type fine pixel detector which will be installed to the layer 2-4 of the ATLAS Inner Tracker (ITk) upgrade. 2) New fine timing resolution detector using avalanche gain technology (LGAD) for future general tracking detector which need timing resolution. 3) A monolithic SOI CMOS detector for future collider experiment as tentative target of ILC vertex detector. All of three development in Japan need precise measurement of the position resolution, detection timing and precise position dependence of efficiency. To achieve this measurement high energy hadron beam is necessary and FTBF facility with 120 GeV proton beam suit well to the requirement of beam condition for our collaboration.

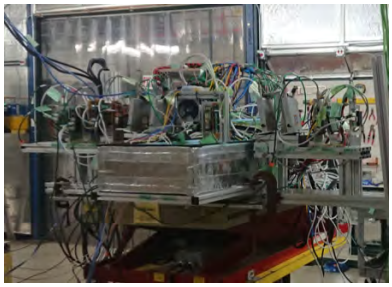

Figure 14: Setup of the ATLAS and LGAD detectors

Setup

Two different set of position measurement detector (Telescope) and Detector Under Test (DUT) are located in MT6.2B and C area.

ATLAS and LGAD setup at MT6.2B

The Telescope is constructed by six layers of ATLAS pixel detector with FE-I4 ASIC (25 μm$\times$ 500 μm pixel size). To obtain better resolution, the device with odd layer number have been rotated by 90 degree. As DUT, LGAD detectors and ALTAS pixel detectors are placed at the middle of telescope. A picture for this setup is shown in Figure 14. A strip type of LGAD detctor was tested at the first time. Some pixel detectors with ATLAS prototype chips (RD53A) have been tested to evaluate the performace of $25\times100\mu m^2$ pixel size.

SOI setup at MT6.2C

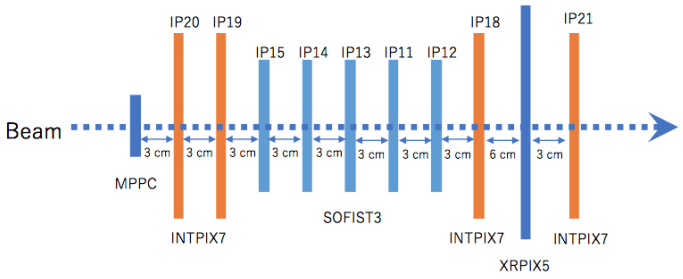

Figure 15: Setup for SOI pixel detector. SOFIST3 is DUT, INTPIX7 is telescope and XRPIX5/MPPC are trigger counter.

The setup of SOI detectors consists of five layers of SOFIST3 and four layers of INTPIX4 sensors as shown in Figure 15 . SOFIST3 is the prototype sensor for the ILC vertex detector and has a pixel circuit for recording hit, timestamp and charge of incident particles. Each pixel has the comparator for signal discrimination and three memories to store up to three hits within 30×30 μm^2. INTPIX7 is the large area SOI pixel sensor with the pixel size 12×12 μm^2. The INTPIX7 sensors were used as the telescope for the SOFIST3. XRPIX5 is also SOI pixel sensor with the pixel size 35×35 μm^2. It is used as trigger counter with region of interest function to increase tracking efficiency.

Results and Publications

ATLAS and LGAD results

For the telescope operation successfully done and resulting 7 μm pointing resolution obtained. A new ATLAS pixel modules with RD53A chip also be tested. RD53A ASIC have 400$\times$192 pixel matrix with 50$\times$50 μm^2 pixel size. Both 50$\times$50 μm^2 and 25$\times$100 μm^2 pixel size semi-conductor sensor is able to flip-chip to the ASIC. The Physics simulation of

ATLAS experiment prefer 25×100 μm^2 pixel size to achive better momentum resolusion in the inner detector especially for the first two layers. On the other hand 25×100 μm^2 pixel size have larger inter pixel capacitance and this results significant cross talk. In the testbeam in FY19, 25×100 μm^2 pixel size pixel detector has been tested. The 30-50% of cross talk has been observed depends on the pixel biasing structure when the comparator threshold set to the charge corresponding to the 1000 electron.

For LGAD sensor, 2×2 matrix pad detector and 80μm pitch strip detector have been tested. The pad detector achieve 30 ps timing resolusion as similar as we evaluated the timing resolution by single diode detector in FY18. The analysis of strip type detectors are still on going.

SOI results

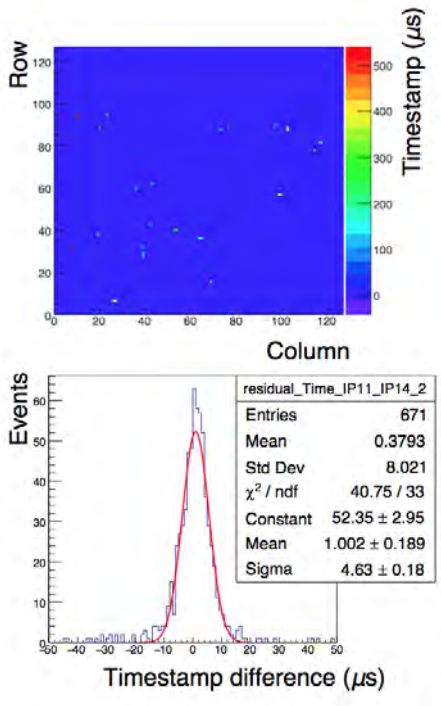

Figure 16: (top) Hit timing in 500 μs store window. (bottom) Timestamp difference between two SOFIST3.

Figure 16 (top) shows hit timing in 500 μs store window, and color differences indicates timestamp of hits. Hit timing difference for evaluating timestamp consistency between two SOFIST3 is shown in Figure 16 (bottom). Standard deviation of gaussian fit is $\sigma = 4.63$ μs. We have extracted 3.29 μs of intrinsic time resolution which divided σ by $\sqrt{2}$.

9 T-1224

J. Metcalfe[1], M. Benoit[2], V. Bhopatkar[1], W. Islam[3], M. Jadhav[1], J. Lambert[4], J. Muse[4], S. Nagasamudram[5], S. Shrestha[5], D. Wilbern[4], W. Wu[5], J. Xie[1], L. Xu[6]

[1]Argonne National Laboratory
[2]Université de Genève
[3]Oklahoma State University
[4]University of Oklahoma
[5]University of Chicago
[6]Brookhaven National Laboratory

Beam Used: 120 GeV Protons
Run Dates: 11/21 - 12/4 2018, 1/16 - 2/5, 3/6 - 3/26, 5/2 - 5/11, 5/20 - 5/25 2019

Motivation and Goals

The top priority for experiment T1224 is to prepare for the ATLAS Inner Tracker (ITk) Pixel Phase II Upgrade. The Large Hadron Collider (LHC) at CERN will upgrade the accelerator and improve the instantaneous luminosity. New tracking detectors are needed to survive the intense radiation environment and will be replaced during the High Luminosity LHC (HL-LHC) Upgrade. The new silicon pixel detector will reduce the pixel size and implement a new Front-End (FE) ASIC designed by the RD53 Collaboration. One of the main goals was to implement the FELIX DAQ system that will be used in ATLAS detector to read out pixels for the first time. The pixel modules will come in a quad configuration with 4 FE chips and 1 sensor. The other main goal was to characterize the performance of the quad modules in order to implement them as telescope planes to replace the previous FEI4 modules, which were on loan. A separate FELIX system was integrated to run with FEI4 modules, MIMOSA modules, and CMOS modules. Tests with the ATLAS CMOS sensors were also continued from the previous year although very limited in scope. Low gain amplifying (LGAD) detectors were also tested as part of the Argonne Electron Ion Collider (EIC) research program.

Setup

The ATLAS Pixel telescope is installed permanently in section 1B. It typically consists of 6 FEI4 based telescope planes. A device under test (DUT) box is inserted in the middle of the telescope planes in order to characterize the tracking performance of the modules. The DUT box can hold up to 4 modules depending on type and configuration. The box

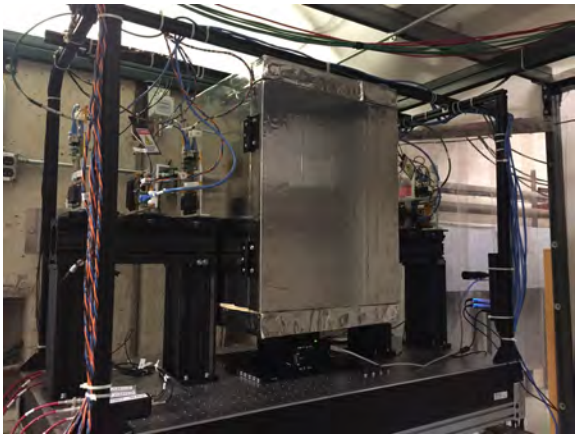

Figure 17: The test beam setup includes 6 planes of pixel detectors and a cold box for the DUT.

has been demonstrated to achieve temperatures down to -25 degC. The setup is shown in Figure 17.

FEI4 Quad Modules

FEI4 quad modules were characterized in order to validate bump bonding in a quad configuration and to gain experience with testing an object similar to the final ITk Pixel modules. Four chips were bump bonded to a single sensor and a flex cable designed at Argonne was glued to the sensor and wire bonded to the FE chips. A number of bump issues were identified on the corners of several modules indicating issues with the processing and the bump vendors. Additionally, the modules were found to have improved performance with cooling and a system to cool the FEI4 quads as telescope planes is under development. Figure 18 shows the FEI4 quad modules.

Spoorthi Nagasamudram, a first year graduate student at the University of Chicago, undertook a project to optimize the telescope performance by tilting the modules. She ran GEANT4 based simulations, implemented the hardware to tilt the modules by designing and 3D printing holders, tested the tilted modules, reconstructed the data, and compared to simulation results. This project resulted in a presentation at the 2019 Fermilab New Perspectives workshop.

FELIX DAQ for FEI4 modules and MIMOSA modules

Weihao Wu and others at Brookhaven National Laboratory (BNL) developed a FELIX DAQ to read out FEI4, MIMOSA, and CMOS modules. The system was installed and

Figure 18: Three FEI4 quad modules are shown as DUT's in the telescope. The third one was tilted to evaluate the improvement in the position resolution.

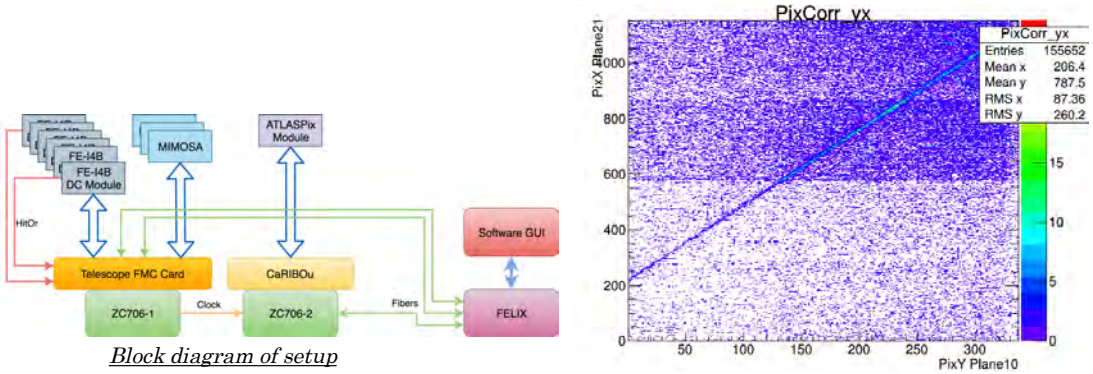

Figure 19: Left: The readout scheme for FELIX with FEI4, MIMOSA, and CMOS silicon pixel modules. Right: The correlation plot between an FEI4 and MIMOSA modules that indicates that the events were successfully combined.

tested for the first time in the test beam. The readout was demonstrated for all 3 types of modules including correlation between each of the 3 flavors. The readout speed was tested at 1.28 Gbps for the ATLAS CMOS modules taking advantage of the high particle counts available at the Fermilab test beam.

FELIX DAQ for RD53A modules

The Argonne group implemented the RD53A Yet Another Rapid Readout (YARR) software into the FELIX framework successfully for the first time. It was integrated into the test beam and a beam spot was observed as shown in Figure 20. Issues were identified to correlate with the other DAQ systems

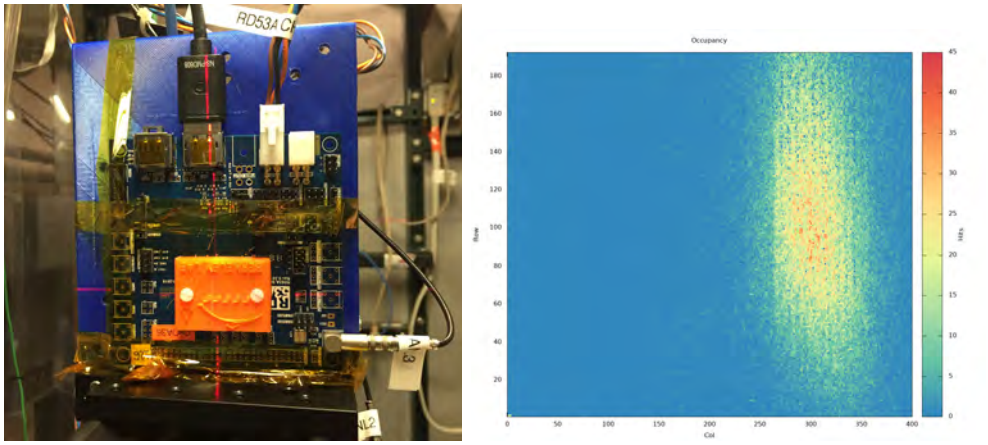

Figure 20: Left: An RD53A module installed in the FTBF. Right: The first beam spot observed with an RD53A module using the FELIX DAQ.

LGAD Sensors

Fast timing silicon sensors are a promising new silicon technology that can reach timing resolution on the order of 10's of picoseconds. Argonne recently joined the effort in testing LGAD sensors for application in the EIC. LGADs obtained from University of California Santa Cruz and BNL were characterized in the test beam using a standalone test configuration. The setup and the timing resolution for one of the sensors is shown in Figure 21.

Publications and presentations:

- *Design, Testing and Improving Performance of a Silicon Pixel-Based Telescope*, Spoorthi Nagasamudram, New Perspectives, Fermilab 2019. https://indico.fnal.gov/event/20381/session/0/contribution/26/material/slides/0.pdf

Papers Under Preparation:

- *Argonne Pixel Telescope* V. Bhopatkar, et al.
- *RD53A Test Beam Characterization with FELIX Data Acquisition* J. Lambert, et al.
- *Timing Characterization of Low Gain Amplifying Detectors with 120 GeV Protons* M. Jadhav, et al.

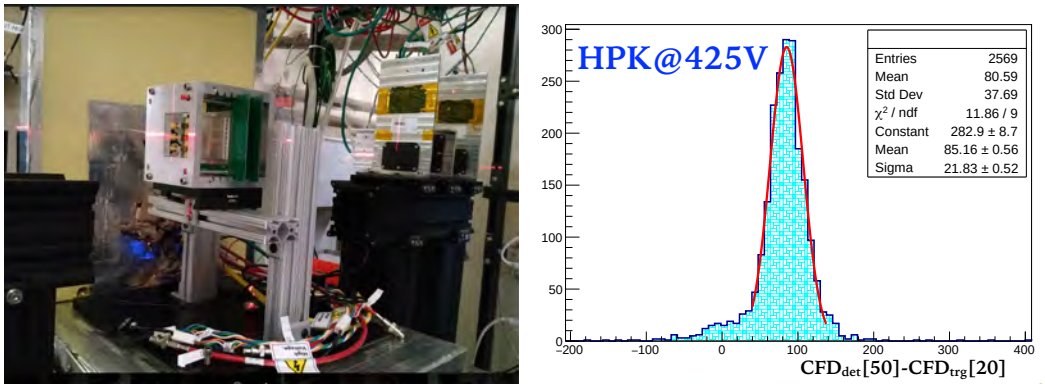

Figure 21: Left: The LGAD test setup in the test beam. Right: The timing distribution is shown based on the difference between the constant fraction discriminator of the trigger and detector planes. The preliminary result corresponds to a timing resolution of 16 ps.

Training

The test beam is an important opportunity to train the next generation of physicists in hardware in order for them to receive a comprehensive understanding of operating a detector system. Figure 22 shows some of the people that have been/will be trained on the Argonne Pixel Telescope.

Figure 22: T1224 group.

10 T-1409 CMS Timing Barrel

T. Anderson[1], M. Arenton[1], P. Barria[1], A. Benaglia[2], O. Cerri[3], B. Cox[1], I. Dutta[3], M. Hermann[4], M. Joyce[1], G. Karaman[4], G. Kopp[5], N. Lu[3], M. Lucchini[5], J. Mao[3], A. Mohammadi[6], L. Paredes[3], C. Pena[3], C. Rude[4], B. Tannenwald[1], C. Wang[3], S. White[1], S. Xie[3]

[1]University of Virginia
[2]INFN-Milano
[3]California Institute of Technology
[4]University of Iowa
[5]Princeton University
[6]Kansas State University

Beam Used: 120 GeV Protons
Run Dates: 11/7-18/11-20/18, 4/17/19-4/30/19, 6/3/19-6/8/19

Motivation and Goals

The goal is to test various LYSO crystal + SiPM layouts in order to reach a goal of measuring MIPs with 30ps resolution. This involves testing different models of SiPMs from different vendors, trying different glues to couple the crystals and SiPMs, tests with the beam incident at different angles, measuring detector response while simultaneously illuminiating multiple bars, and testing the design of the readout electronics. Ultimately this R&D will inform the design and production of the timing layer planned for the HL-LHC upgrade of the CMS detector.

Setup

The test setup is placed behind the pixel telescope in MT6 Section 1 along the beamline. The April and June runs used the cold box shown in Figure 23.

Alignment with the pixel telescope (provided by FNAL) was necessary as a reference on the positions measured by the LYSO crystals. Single bars were coupled to SiPMs and wrapped in teflon tape before being placed in the beamline (see Figure 24. Five-bar setups as well as pre-packed matrices of 16 bars were also tested.

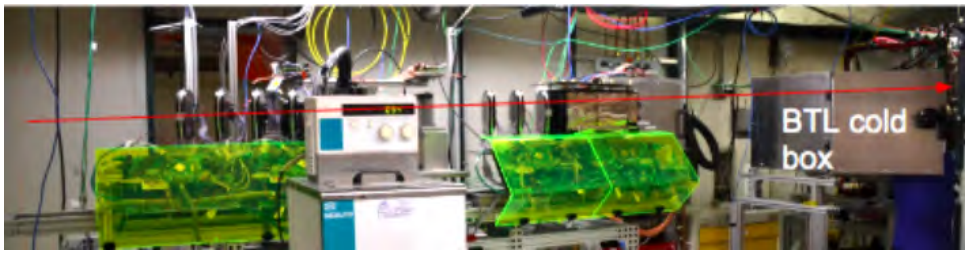

Figure 23: Testbeam setup in beam enclosure with pixel telescope

Figure 24: Example of test-beam setup for telfon-wrapped LYSO bars with dual SiPM readout.

Results and Publications

The previous year of testbeam activities have enabled us to reliably obtain a 30 picosecond time resolution for MIPs measured by our LYSO+SiPM sensors. Figure 25 shows the time resolution as a function of the position in the LYSO bar for each individual SiPM and for their combination. The time resolution is observed to be independent from the hit position in the bar.

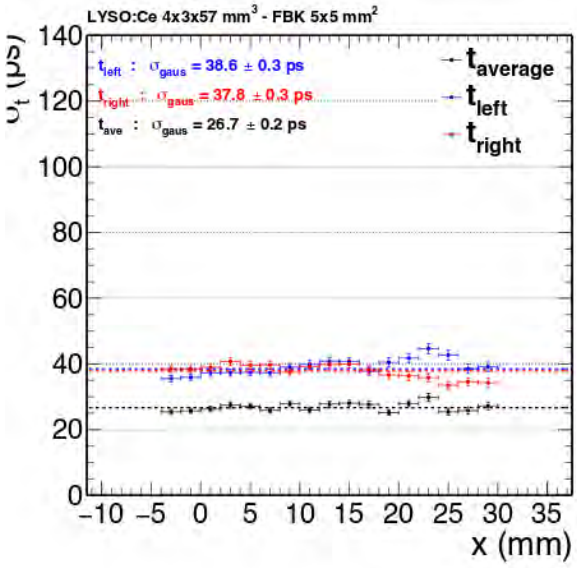

Figure 25: Measured time resolution for MIPs as a function of the position along the LYSO bar. The resolution is flat across the bar, and the resolution obtained using measurements from both SiPMs reaches the goal of 30 picoseconds.

Figure 26 shows the time resolution as a function of the crystal thickness traversed by passing MIPs. Simulation predicts a better time resolution for thicker crystals, and the confirmation of this behaviour is important since the full detector in CMS will utilize material levelling as a function of eta to produce a uniform timing response throughout the detector. Addtional measurements of the time resolution as a function of the MIP incidence angle have confirmed expectations from simulation. Additional tests from the June testbeam are helping to improve the development of a second version of the readout electronics to be used for the full detector in CMS.

Many of the results produced from Fermilab testbeams have been included in the Technical Design Proposal for the CMS MTD.

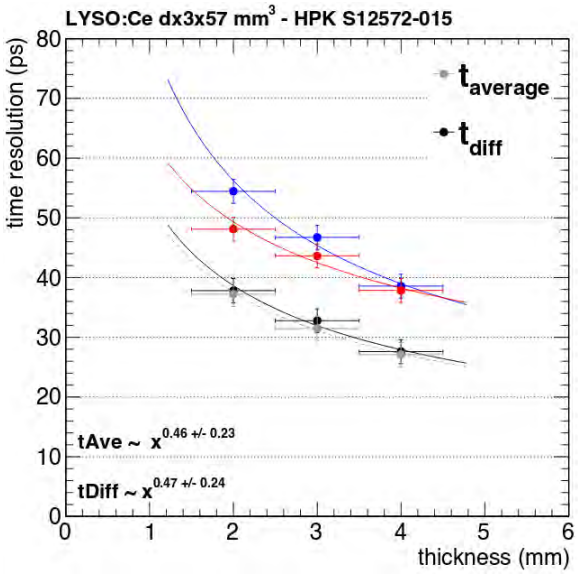

Figure 26: Measured time resolution as a function of the crystal thickness traversed by passing MIPs. As expected, thicker crystal depths lead to a better observed time resolution.

11 T-1409 CMS Timing Endcap

A. Apresyan[1], C. Rogan[2], M. Obertino[3], R. Heller[1], S. Xie[4], C. Pena[1], N. Minafra[2], A. Ovcharova[5], M. Hussain[6], T. Wamorkar[7], F. Siviero[3], T. Isodori[2], M. Lazarovitz[2], A. Abreu[2], A. Koziol[8], D. McGraw[2]

[1]Fermilab
[2]University of Kansas
[3]Torino
[4]Caltech
[5]University of California Santa Barbara
[6]University of Chicago
[7]Northeastern
[8]AGH University of Science and Technology, Krakow

Beam Used: 120 GeV Protons
Run Dates: 11/7-18/11-20/18, 4/17/19-4/30/19, 6/3/19-6/8/19

Motivation and Goals

During test beams at the FTBF in 2019 we studied several new prototypes of silicon timing detectors for advanced tracking applications in high energy physics. The goals of these measurements were to establish a radiation hard technology capable of measuring the arrival time of minimum ionizing particles (MIP) with 30-40 ps resolution. A target application for these sensors is the CMS MIP Timing Detector Phase 2 Upgrade (MTD) to be installed for High Luminosity LHC (HL-LHC).

At the HL-LHC an average of 140-200 pileup interactions will occur over a spread of approximately 200 ps. The spatial overlap of tracks and energy deposits from these collisions will lead to a substantial rate of false pileup association with the primary interaction and degrade the event reconstruction. Precision time stamping at the order of 30-40 ps for all charged particles enables isolating the hard scatter from pileup interactions and enables a reduction in effective pileup by factor of 4-5, maintaining performance comparable to the current Phase 1 CMS detector despite the more challenging environment. This enhancement translates into 20-30% increase in di-Higgs signal efficiency (depending on its decay channel), which increases discovery sensitivity almost as an equivalent increase in the integrated luminosity.

At the FTBF, several silicon low gain avalanche detectors (LGADs) were studied as prototypes for the high radiation Endcap Timing Layer (ETL) section of the CMS MTD. LGADs fabricated by Hamamatsu (HPK) and Fondazione Bruno Kessler (FBK) were characterized, with the main goals of establishing timing performance at a precision of 30-40 ps even after large fluences beyond 10^{15} neq/cm^2, with good uniformity across large-area sensors.

Setup

The ETL LGAD characterization setup resides in a mobile rack immediately downstream of the FTBF silicon tracker in Section 6.1A (Fig 27). At the top of the rack is the cold box, which can host up to 5 LGADs mounted on cooling blocks, as well as the Photek MCP which serves as a time reference with 10 ps resolution. These devices can move up to 5-10 cm transverse to the beam to align sensors with the beam as well as with elements of the FTFB tracker. Immediately underneath the cold box are all of the instruments necessary for control of motor stages, thermal monitoring, and the low voltage supplies powering analog amplifiers. Further down the rack is the red CAEN 8-channel HV supply, which provides the bias voltage for the LGADs and the MCP, and the DAQ PC which manages the local instruments and enables complete control of the setup remotely. Analog signals are sent to a high resolution Keysight oscilloscope via a high performance multiplexer, which allows for switching between up to 24 channels remotely without interrupting the beam. The oscilloscope acquisition is optimized for the burst structure of the test beam

and can capture up to 130k events in a single 4 second spill with effectively no dead time, and subsequently write the waveforms to disk during the 56 second inter-spill period.

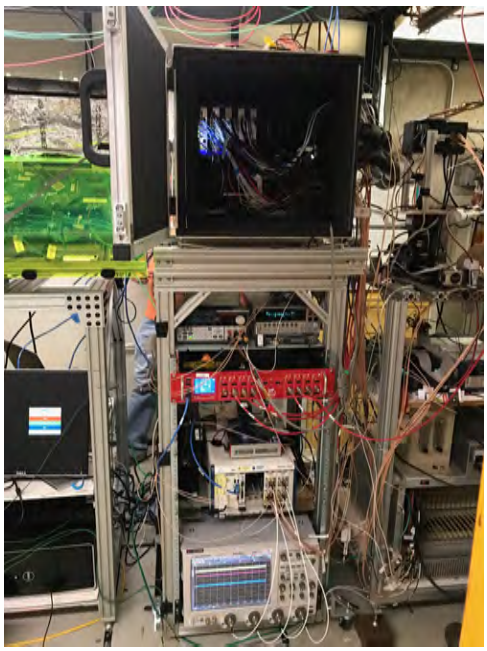

Figure 27: Photo of silicon timing detector characterization facility in Section 6.1A.

Results and Publications

Two successful ETL test beam campaigns were carried out during the 2018-2019 season, and two more are planned for the coming year. In November 2018, prototype LGADs from FBK were characterized, with a focus on studying their performance after irradiation. Using the test beam, we were able to establish that these devices maintain close to 40 ps time resolution even after a fluence of 1.5 x 10^{15} neq/cm^2, the dose expected in the innermost regions over the full life of the ETL (Fig 28. Achieving this performance for the full life of the detector represents a major milestone for the CMS ETL project.

In April 2019, the ETL test beam effort focused on characterization of HPK prototype LGADs, including measurements of several irradiated large-area 16-channel LGAD arrays for the first time with MIP signals. The FTBF offers unique capabilities for sensor uniformity characterization, thanks to the excellent proton localization provided by the FTBF tracker. Example maps of signal amplitude and time resolution uniformity are shown in Fig 29. These studies have enabled us to demonstrate the feasibility of producing uniform, large area LGADs, a crucial step for on the path towards building the CMS ETL.

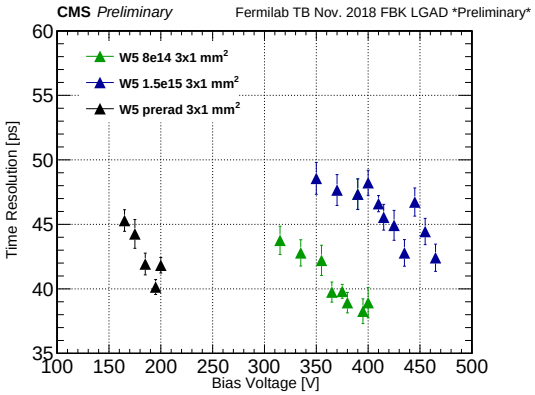

Figure 28: Timing performance of FBK UFSD3 sensors (1x3 mm^2 single pads) as a function of bias voltage at increasing fluences.

Results from these campaigns were featured in the CMS MTD Technical Design Report, and shown at conferences including the 34th RD50 workshop and the 2019 Meeting of the American Physics Society Division of Particles and Fields. These results will be included in a publication including other characterization measurements based on the same protoypes, expected to be published early in 2020.

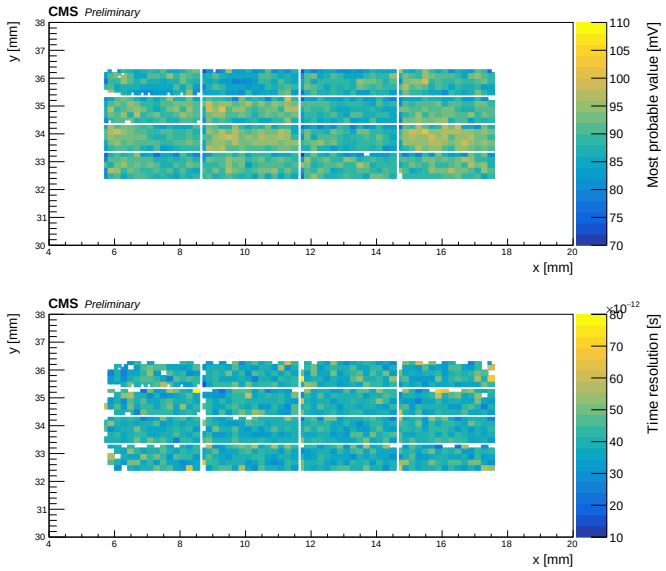

Figure 29: Map of most probable MIP response (top) and time resolution (bottom) across the surface of non-irradiated HPK 3.1 4x4 array (1x3 mm^2 pads), at bias voltage 195 V and temperature -18 C. The time resolution is

12 T-1429 Performance Study of MPGD Based Detectors with Zigzag Pad Readout

S. Aune[1], B. Azmoun[2], W. Fan[3], A. Kiselev[2], I. Mandjavidze[1], C. Perez-Lara[3], M. Purschke[2], M. Revolle[1], M. Vandenbroucke[1], C. Woody[2]

[1]CEA Saclay
[2]Brookhaven National Laboratory
[3]Stony Brook University

Beam Used: 120 GeV Protons
Run Dates: March 20 - April 2, 2019

Motivation and Goals

Highly interleaved zigzag patterned readout pads may be specially tailored to significantly enhance charge sharing over more standard readout pad designs used for many MPGD applications. The goal of this beam test was to systematically study the dependence of the detector performance, including the spatial resolution, on the parameters that define

the geometry of zigzag shaped charge collecting anodes. More specifically, the detector response was measured for 100 different zigzag readout designs coupled to various MPGD avalanche schemes, including GEM, Micromegas, and μRWELL.

Setup

Eight individual detector chambers, each equipped with a multi-zigzag readout plane (corresponding to a total of roughly 4500 electronics channels) were simultaneously scanned in the 120GeV primary proton beam using an XY positioning stand, seen in Figure 30. Tracking information from the FTBF silicon telescope in the 6.1A area was also employed to precisely determine the spatial resolution.

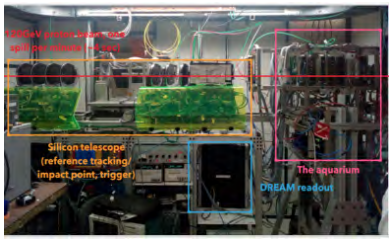

Figure 30: Beam test setup in the 6.1A area at FTBF. The aquarium holds all 8 detector chambers, with the silicon tracker to the left and the DREAM front end electronics at the bottom.

Results and Publications

After scanning the parameter space of the zigzag geomtery, we have identifed optimal parameter sets for specific detector configurations that correspnd to excellent spatial resolution and a uniform detector response, with no need for so-called pad response functions. Figure 31 shows the geometric parameterization for a generic zigzag and a 50m resolution achieved for a realtively coarse, 2mm pitched readout. Figure 32 shows the unformity of response for an optimal (top) and a suboptimal zigzag design (bottom).

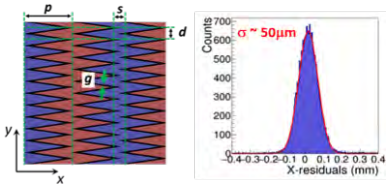

Figure 31: Zigzag geometry and the residual distribution for an optimal parameter set.

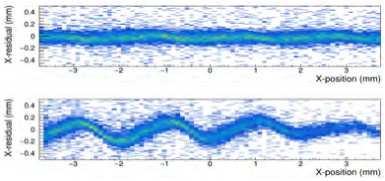

Figure 32: Detector response from two different zigzag readout designs.

13 T-1439

Yasuyuki Akiba[1,2], Kai-Yu Cheng[3,2], Edmond Desmond[4], Takashi Hatchiya[5,2], John Haggerty[4], Shoichi Hasegawa[6,1], Takashi Kondo[7,1], Chia-Ming Kuo[3], Itaru Nakagawa[1,2], Rachid Nouicer[4], Cheng-Wei Shih[3,2], Ayaka Suzuki[5,1], Takahito Todoroki[2], Rui Xiao[8,2], and Wei Xie[8]

[1]RIKEN
[2]RIKEN-BNL Research Center
[3]National Central University
[4]Brookhaven National Laboratory
[5]Nara Women's University
[6]Japan Atomic Energy Agency
[7]Tokyo Metropolitan Industrial Technology Research Institute
[8]Purdue University

Beam Used: 120 GeV Protons
Run Dates: June 10 - 21, 2019

Motivation and Goals

sPHENIX is a proposal for a major upgrade to the PHENIX experiment at RHIC capable of measuring jets, photons, and Upsilon states to determine the temperature dependence of transport coefficients of the quark-gluon plasma. The detector needed to make these measurements require electromagnetic and hadronic calorimetry for measurements of jets, a high resolution and low mass tracking system for reconstruction of the Upsilon states, and a high speed data acquisition system.

The INTermediate Tracker (INTT) is one of the particle of sPHENIX tracking .detectors which consisted of MVTX, INTT, and TPC. The INTT detector consists of 2 barrel layers of silicon strip detectors (radius : ~ 7 and ~ 10 cm) covering an acceptance of pseudorapidity within $\pm$ 1.1, and a 2π in azimuth. The INTT prototype was first tested at the Fermi National Accelerator Laboratory (FNAL) Test Beam Facility as experiment T-1439 in

March 2018. In this document, the summary of the 2nd beam test of the INTT prototype executed in May 2019 is reported.

Setup

The INTT telescope consists of four silicon strip half ladders mounted in a dark box as shown in the left panel of Fig. 33. Each half ladder consists of one flexible circuit boards called High Density Interconnect (HDI). Each HDI (approximately 350 um thick, 400 mm long, and 35 mm width) provides the slow control, power, and bias input lines as well as slow control and data output lines. The HDI was manufactured and tested by Yamashita Material co. The HDI carries two AC coupled silicon strip sensors' single side (with $26 \times 128 = 3328$ readout channels in total) located in the middle of the HDI, and 13 FPHX chips in each side of the sensors. The FPHX chip consists of 128-channel front-end ASIC, and was designed by Fermilab for the PHENIX/FVTX detector. The chip was optimized for fast trigger capability; a trigger-less data push architecture, and low power consumption (64 mW/chip). Each half ladder is mounted on one support structure (stave) made of Carbon-Fiber-Carbon composite carrying a liquid cooling tube. Each ladder is readout through an extender cable. The HDI ends was connected to a 1.2m long prototype extender cable with a 20cm conversion cable which is connected at the other end to a FVTX ROC (Readout Card) used in PHENIX/FVTX previously.This is the first time to test the full read out chain under the beam circumstance as shown in the right panel in Fig. 33.

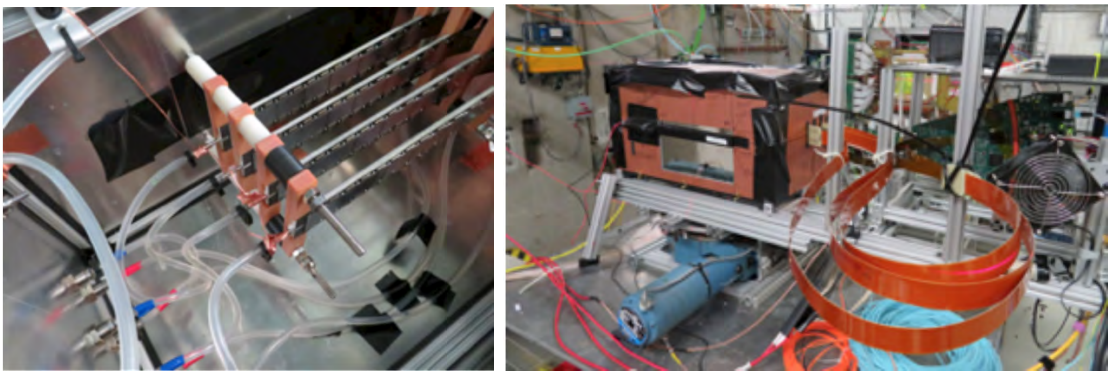

Figure 33: (left) The INTT telescope consisted of 4 silicon strip half ladders mounted in a dark box. (right) Full setup including the 1.2m long prototype bus extender cables and readout electronics card.

Results and Publications

In oder to evaluate the performance of INTT detector under various conditions, following measurements were executed.

- Timing scan to time-in
- ADC fine scan over wide range
- DAC0 threshold scan for optimization of the efficiency and S/N ratio
- Position dependent efficiency scan
- Horizontal angle dependency scan to study energy deposit in different effective thickness
- Vertical angle dependence to develop charge sharing between adjacent strips
- Rate dependent performance
- S/N and efficiency comparisons with and without the bus extender cable
- Monitoring eye diagram of the high frequency differential signal transmission with the bus extender

Shown in the left panel of Fig. 34 is the ADC spectrum of a given chip around the beam spot area. Series of measurements with the finest DAC bin setting of 3 bits ADC, but slightly shifted ADC range are concatenated into one histogram to span the wide ADC range. Clear separation between the low ADC and MIP peak around 120 channel is observed. The typical hit distributions of 3 ladders observed at 120 GeV proton beam are displayed in the right panel of Fig. 34. The y-axis and x-axis of the plot correspond to the number of hits, and silicon strip number, respectively. Each panel represents the distribution for the chip of a corresponding layout. Histograms surrounded by red dashed box is the chips in the region where being illuminated by the beam spot. The beam spot size was larger compared to the one in the 2018 beam test. To summarize, we accumulated INTT telescope data in various conditions in order to evaluate its performance in more realistic operation environment. Analysis results are to be published from NIM article within a year or so.

Acknowledgements: We would like to thank the management and technicians of the Fermilab Test Beam Facility for their supports during our experiment T-1439 in May 2019.

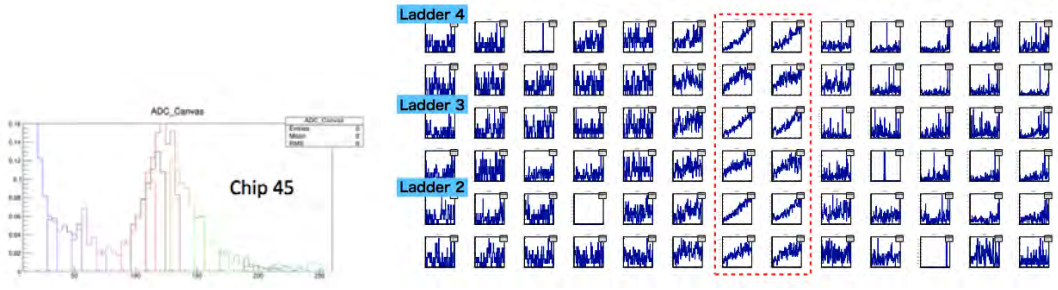

Figure 34: ADC distribution observed in one of the readout FPHX chip around the beam spot.

14 T-1441

C. Dean[1], M. Durham[1], H. van Hecke[1], G.J. Kunde[1], X. He[2], J. Huang[5], X. Li[1], Z. Li[1], S. Lim[3], M.X. Liu[1], Y.C. Morales[1], C. O'Shaughnessy[1], M.L. Purschke[5], A. Raymer[1], C. da Silva[1], W. Sondheim[1], X. Sun[2], M. Taylor[4], A. Tkatchev[1], S. Uemura[1]

[1]Los Alamos National Laboratory
[2]Georgia State University
[3]University of Colorado
[4]Massachusetts Institute of Technology
[5]Brookhaven National Laboratory

Beam Used: 120 GeV Protons, 5 GeV electrons
Run Dates: May 20-25, June 17-22 2019

Motivation and Goals

The primary goals of the test beam are to test the MVTX readout chain with final frontend (RU) and backend (FELIX) electronics with the ALICE production sensor staves and demonstrate the MVTX tracking performance at the sPHENIX trigger rate of 15kHz.

Setup

Figure 35 shows the MVTX telescope setup at Fermilab, with a negative pressure cooling system. Figure 36 shows the schematics of the readout and control chain.

Figure 35: MVTX Telescope Setup at FTBF. A 4-stave telescope assembly was used at Fermilab to verify the detector tracking performance with the latest near final readout electronics and high-speed data cables. and production sensor staves.

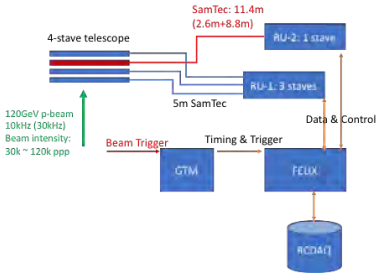

Figure 36: Schematics of the electrical system

Results and Publications

We succesfully carried out the test beam runs. Preliminary results show that the readout chain can take data at the desired sPHENIX trigger rate of 15kHz without errors (typical data taking trigger rate 30kHz, stress-tested upto 300kHz, the maximum available rate at FTBF). The hit spatial resolution is better than 5um, with efficiecny great than 99.5

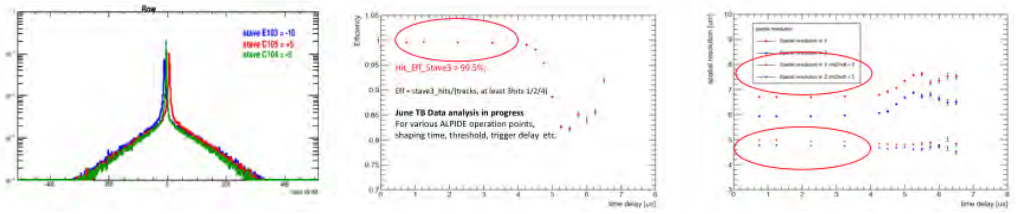

(a) (b) (c)

Figure 37: Panel 37a: raw hit z position distributions of 3 staves relative to the 1st reference stave, with 120GeV p-beam; Panel 37b: Hit efficiency vs trigger delay, 99.5% or higher; Panel 37c: Hit resolution vs trigger delay, 5μm.

15 T-1450

M. Chiu[1], E. May[2], S. Nelson[3], C. Scarlett[3], J. Xie[2]

[1]Brookhaven National Laboratory
[2]Argonne National Laboratory
[3]Florida A&M University

Beam Used: 120 GeV Protons
Run Dates: March 20 - April 2, 2019

Motivation and Goals

As part of the eRD14 consortium developing PID detectors to be used at the EIC, we are developing pixelated LAPPD-style micro-channel plate PMTs (MCP-PMTs). Pixelated MCP-PMTs are required for imaging detectors such as RICH or DIRCs, and we have devised a novel capacitively coupled readout which allows any pixel design to be used. We tested the rate capability and position resolution of square pixel pads from 2x2 to 4x4 mm^2 in size, with signals generated from a dual MCP stack.

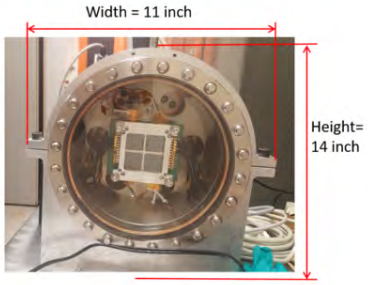

Figure 38: ANL Pixelated 6x6 cm^2 MCP-PMT

Setup

The ANL demountable is a stack of a Boro33 window with an Al photocathode, 2 Incom MCPs, and a pixelated PCB to form a MCP-PMT. The MCP-PMT stack is housed inside a vacuum chamber, as shown in fig. 1. The PCB consisted of 4 sections of 2x2, 3x3, 4x4, and 5x5 mm^2 pads, with 16 channels arranged in a 4x4 square configuration in each section. The MCP-PMT was arranged in the beam-line with trigger scintillators in front and behind, and read out in coincidence with the FTBF MWPCs 1 and 2. Data were taken for the 2x2 to 4x4 mm^2 pads.

Results and Publications

To determine the position resolution, we took the difference between the projection from the MWPC hits onto the MCP-PMT plane, and the position determined by the MCP-PMT pixel hits. The difference between the MWPC and MCP-PMT determined positions is shown in fig. 2 for the 3x3 mm^2 pads, resulting in a sigma of 0.95 mm, consistent with expectations. The resolutions for the 2x2, 3x3 and 4x4 mm^2 pad runs were 1.4, 0.8 and 1 mm, respectively. This was the first measurement of LAPPD-style MCP-PMTs with pixelated capacitively-coupled readout through a glass interface. This shows that one can design a customized pad readout design for their MCP-PMT applications.

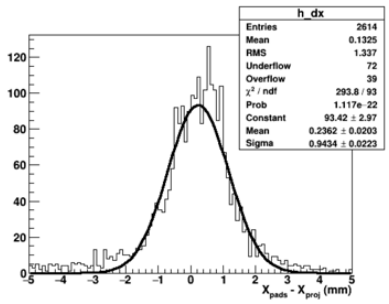

Figure 39: Difference between the projected hit position as determined by the MWPCs, and the position determined by the MCP-PMT pixels.

16 T-1473

T.K. Hemmick[1], K. Delmelt[1], T. Sakaguchi[2], J. Huang[2]

[1]Stony Brook University
[2]Brookhaven National Laboratory

Beam Used: 120 GeV Protons
Run Dates: June 10 - 21, 2019

Motivation and Goals

sPHENIX is a future experiment to be run at the BNL RHIC facility. The principle tracking device will be a compact (1.6 meter diameter; 2 meter length) Time Projection Chamber. The unusual characteristic of the sPHENIX TPC is that the device is designed to deliver excellent position & momentum resolution without the usual requirement of dE/dx measures.

The key is that we choose a low diffusion (cold) gas (Ne:CF_4 50:50) coupled to a zig-zag pad plane readout of a quad GEM-stack. The quad GEM-stack allows one to run in a low Ion Backflow mode (minimizing space charge distortion). This experiment was used to confirm the position resolution goals and demonstrate stable working in the low IBF configuration.

Figure 40: sPHENIX TPC setup.

Setup

The TPC prototype was mounted to a motion table that allowed the device to be moved transverse to the beam and also rotated around the vertical and horizontal axis. This configuration allows us to measure the position resolution (the TPC has 16 rows of digitization

and internally self-calibrates) as a function of drift length. Position resolution can be summarized as two terms; one drift length dependent and the other not: $\sigma_{tot}^2 = \sigma_{pad}^2 + \frac{D^2}{N_{eff}} L$. The diffusion constant, D, has well known values with and without magnetic field. σ_{pad} and N_{eff} are the intrinsic resolution of the pad plane and the effective number of electrons, respectively and must be determined by experiment. A plot of σ_{tot}^2 vs. L yields both unknowns and allows a calculation of expectations of the field-on performance of the TPC. This measurement was the principle goals of the run. We also took special runs with:

- High occupancy via incompletely contained electron showers
- High eta tracks (rotation about vertical axis)
- Inclined tracks (rotation about horizontal axis).

Furthermore, this years run used, for the first time, prototype electronics that would be used in the real sPHENIX experiment.

Results and Publications

The plot in Figure 41 is our most important result. Here the position resolution is plotted as a function of drift length. The dots are the field-off data. The line is the result of the fit to data scaled by the known diffusion constants with and without magnetic field.

We see that even for a full meter of drift the the sPHENIX TPC can be expected to have a position resolution better than 150 m. This is a spectacular result.

Not shown here are the resolution for all other aspects of running, each of which was 100% successful.

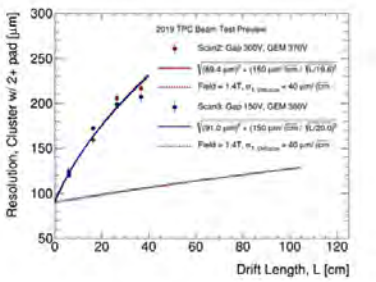

Figure 41: Resolution Measurement. The dots are online measurements with no field and the lower line is scaled by diffusion to yield expected performance.

17 T-1516 CMS HGG-BH Tests

J. Freeman[1], D. Lincoln[1], L. Uplegger[1], S. Uzunyan[2]

[1]Fermilab
[2]Northern Illinois University

Beam Used: 120 GeV Protons
Run Dates: July 1-5, 2019

Motivation and Goals

CMS HGCal upgrade Hadron Calorimeter will be built using small scintillator tiles with SIPM optical transducers. It is important to measure light yield, uniformity, and effect of details of the materials and wrapping technologies. This experiment will explore these issues.

Setup

A small dark box was attached to a computer-controlled XY stage, shown in Figure 42. The box could then be positioned relative to the beam. 2 layers of silicon strip tracker were fixed to the support and so remained stationary relative to the beam. Scintillator trigger counters were downstream from the darkbox. Tile/SIPM was placed in the dark box and read out via DRS4.

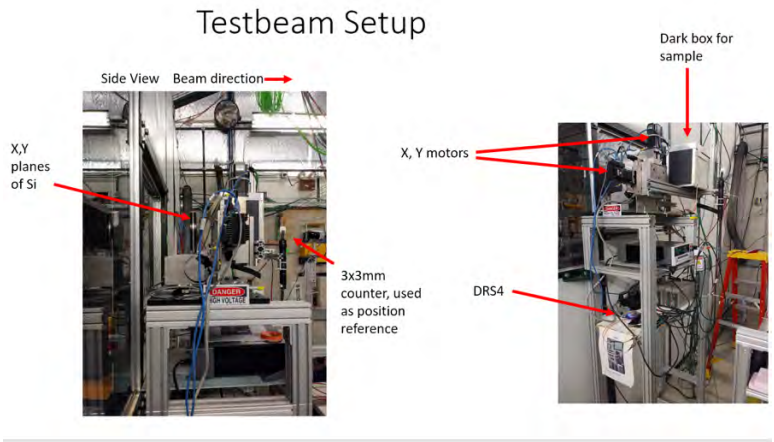

Figure 42: Experimental setup for T1516.

Results and Publications

Over 200 data runs were taken with a number of configurations. Figure 43 shows results from a calibration run using a low light yield configuration, so the photo-electron peaks from the SIPM are more visible. The bottom left side of the figure shows a uniformity plot where the average response is shown vs position. The XY position was determined using the Si strip detector. A reduced LY in the middle of the tile is due to a large dimple cut from the scintillator to accommodate the SIPM. Details of the size of the dimple are part of this testbeam study. Figure 44 shows preliminary results on tile light yields for different scintillators and wrappings. Results from these studies will have direct impact on the HGC calorimeter design.

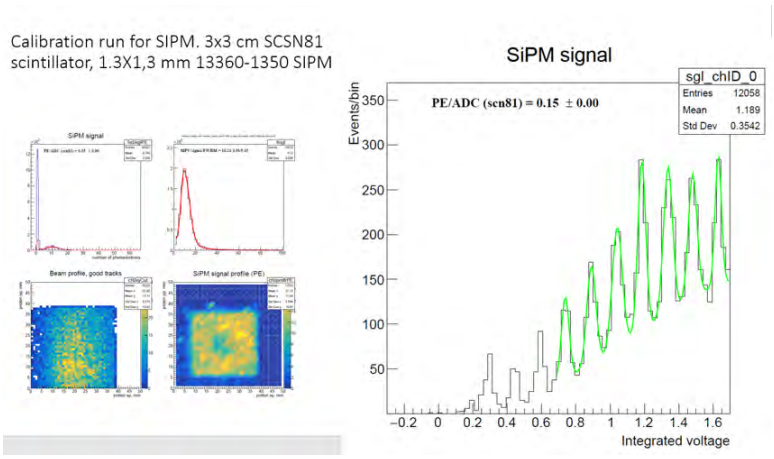

Figure 43: Results from calibration run. The lower left scatter plots show beam profile, leftmost, and scintillator tile light yield in photoelectrons. This tile had artificially low light yield to add in calibration of photoelectrons. (Tile SCSN81tvk) The right-hand plot shows photoelectron fitting. The first 10 photoelectron peaks are clearly visible. PE gain is calculated using this fitting.

Beam Tests:: 120 GeV protons, FTBF, May 10 – Jul 05, 2019
1.3x1.3mm2 SiPM, SN 30119, Vop=54.5V

Tile	MPV, L+G fit	FWHM	Mean (L+G fit)**	Mean (hist)
EJ208esr	35.5	18.3	35.8 +/- 0.1	40.7
EJ200esr	32.7	16.0	32.0 +/- 0.1	37.3
EJ262esr	32.5	15.9	31.9 +/- 0.1	37.6
SC301esr*	22.7	13.2	22.7 +/- 0.1	28.1
SC307esr*	21.8	13.7	21.5 +/- 0.2	27.5
Calice Tile	17.3	11.8	17.3 +/-0.1	22.0
SCN81tvk	10.1	9.3	9.4 +/- 0.1	12.7

Figure 44: Light output (in calibrated photoelectrons) for various types of scintillator material. All tiles were 3cmx3cm by 3mm thick and wrapped in ESR reflector (except for a low light yield calibration tile, SCSN81tvk, wrapped in Tyvek to reduce light yield.). The same SIPM operating at the same voltage viewed the tile. The SIPM was Hamamatsu 13360-1350 type SN 30119. (Preliminary results.)

18 T-1564 LHCb Upstream Tracker

S. Blusk[1], J. Wang[1], S. Ely[1], K. Kim[1], Z. Li[1], M.Wilkinson[1]

[1]Syracuse University

Beam Used: 120 GeV Protons
Run Dates: March 6 - 19, 2019

Motivation and Goals

The goals of the testbeam are to validate the performance of the new SALT ASIC v3.0 for the LHCb UT tracker using a production sensor. We aim to demonstrate the full functionality of the SALT v3.0 ASIC, and measure the signal-to-noise ratio and efficiency for a unirradiated UT sensor, and a maximally irradiated sensor.

Setup

The sensor and readout electronics were placed in an aluminum box to provide a dark environment and EM shielding, and setup was placed in the center of the FTBF telescope, shown in Figure 45. Protons of 120 GeV/c momentum tracked using the FTBF silicon strip telescope to provide the expected position that they protons passed through our

detector under test (DUT). By comparing the recorded hit information in the DUT with the expectations from the tracking system, the distribution of collected charge was measured as well as the DUT efficiency.

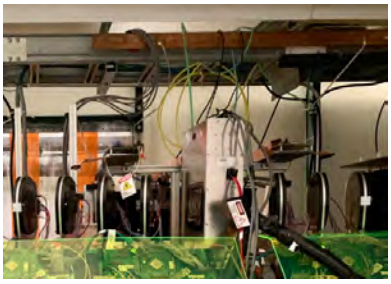

Figure 45: Experimental setup for T1564.

Results and Publications

Figure 46 shows the collected charge on the unirradiated UT sensor with a fit to a Landau distribution superimposed. Figure 47 shows the UT hit efficiency as a function of the inter-strip position. The interstrip position is determined by taking each strip, and normalizing it to unit width, where zero means the proton hit directly on top of the strip N, and -0.5 (+0.5) correspond to half-way between strip N-1 (N+1) and strip N.

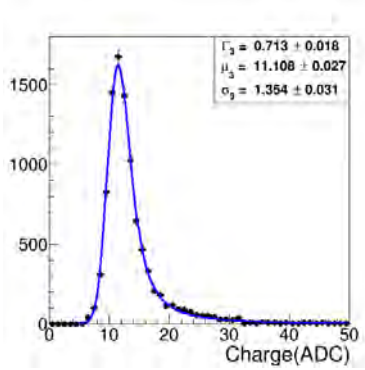

Figure 46

Using an independent measurement of the noise of about 0.9 ADC counts, we infer a signal-to-noise ratio of about 12. A hit efficiency of 99% is obtained. This efficiency is lower than our expectations due to known issues with our testbeam DAQ system. In the end, we expect to obtain an efficiency of at least 99.5%.

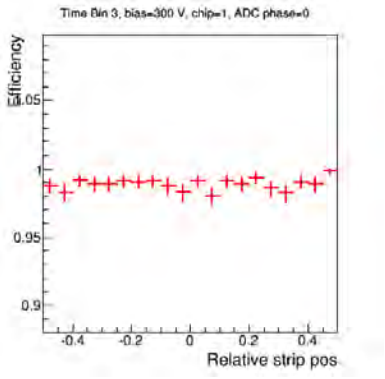

Figure 47

For the irradiated sensor (not shown) the signal-to-noise ratio was measured to be about 10% lower than the unirradiated sensr, consistent with previous test beam results.

The results of the testbeam have validated that the SALT v3.0 ASIC functions as intended, and meets our specifications. As a result, the full production has since been launched.

19 T-1575

M Murray[1], M Nickels[1], Q Wang[1], R Longo[2], C Lantz[2],
T Zhang[2], Y Kulinich[2], S Yang[2], Sean Preins[2], A Mankolli[2],
J Bryant[2], R Karanam[3], Z Citron[3], and E Adams[4]

[1]University of Kansas
[2]University of Illinois, Urbana Champaign
[3]Ben-Gurion University
[4]University of Maryland

Beam Used: 120 GeV protons and 30 GeV electrons
Run Dates: July 1-6, 2019

Motivation and Goals

The Joint Zero Degree Calorimeter project seeks to develop compact radiation hard ZDCs for the ATLAS and CMS experiments during Run 3 and Run 4 of the LHC. These calorimeters will use tungsten as an absorber and very radiation hard fused silica rods as the active medium. The rods will produce Cerenkov light which will be collected by photomultipliers. For Run 4 the available width of the ZDCs will be reduced to 5cm. The purpose of this beam test was to study the shower containment of the electromagnetic section of the ZDCs.

Setup

The ZDC was placed upon the movable, X, Y table in the MTest line 6.2, see Fig. 48. The beam was defined by the logical AND of the S1, S2 and S3 scintillators supplied by the facility with two cross scintillators supplied by our group. The ZDC was aligned with the beam line using the laser alignment supplied by the facility. The two crossed scintillators were then aligned using servo motors. The ZDC was divided into 4 divisions in X and 2 in depth.

Data were taken from July 1^{st} to July 6^{th} 2019 using our own data acquisition system. The principle beams were 30 GeV electrons and 120 GeV protons. The MTest C1 Cerenkov was used to separate electrons from pions and kaons/protons. This Cerenkov has two mirrors that focus light produced at different angles onto two phototubes. Figure 49 shows a scatter plots of the signals from the inner and outer phototubes. Distinct regions corresponding to electrons, pions and protons can be seen. By using two dimensional cuts it was possible to select different particle types. By moving the table it was possible to scan the beam over the face of the detector. By changing the orientation of the ZDC it

Figure 48: The electromagnetic section of the ZDC, tilted at 45^o.

was possible to change the inclination of the beam on the face of the ZDC. Two different configurations of the ZDC were tested, one with 4mm thick tungsten plates and the other with 2mm plates.

Analysis and Results

A data analysis framework, JZCapa, https://urldefense.proofpoint.com/v2/url?u=https-3A__gitlab.engr.illinois.edu_rlongo_JZCaPA&d=DwIGaQ&c=gRgGjJ3BkIsb5y6s49QqsA&r=RgRIj_yBMBH-vEWveCTEYA&m=UUubpCymtdSxhtJaXtRDGp3gyUaWntVSaox2b-7HPsg&s=j_WhS46Ip-IuOB27oYnqVTJoKW-dAv-4bJy6ceTLRR4&e= has been written but a full analysis has not yet been completed. However from online analysis it is clear that the horizontal and vertical scans show a very uniform response to within a few millimeters of the edge of the detector. Also, as expected the signal is larger when the beam hits the ZDC at 45^o and when using 2mm rather than 4mm tungsten plates. The light yield was less than we hoped. We are planning to reduce the length of the air-core light guide and develop

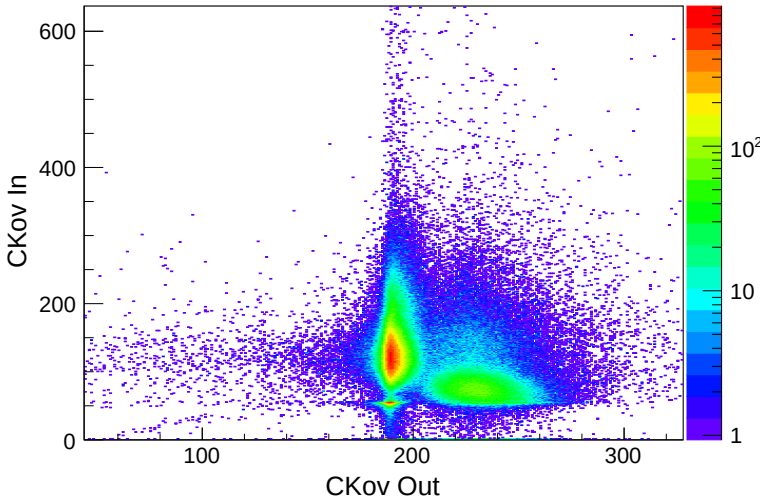

Figure 49: Scatterplot of the inner and outer PMT signals from the first MTest Cerenkov for 30 GeV beam. Different regions of the plots correspond to electrons, pions and protons.

a modified Winston cone geometry to minimize the number of reflections in the detector. The results of this test beam will be used in a proposal for identical ZDC for ATLAS and CMS in Run 3. We plan to submit this proposal in early 2020.

20 LAPPD-TOF Phase 0

[1]E. Angelico[1], B. Adams[1,2], F. Clark[1], A. Elagin[1], H. Frisch[1], M. Popecki[1,2], E. Spieglan[1]

[1]University of Chicago
[2]Incom Inc.

Beam Used: parasitic, outside of enclosure, downstream of MT6.2 pion dump
Run Dates: May 14 - June 7 (intermittent since Feb.)

Motivation and Goals

This project is a first test of measuring charged particles with the commercially-produced Large Area Picosecond Photodetectors (LAPPDs) now available from Incom Inc. Two LAPPDs placed in succession can precisely measure the time-of-flight (TOF) of charged particles by detecting Cherenkov light produced in the detector window or coupled radiators. With picosecond level timing resolution and multiple LAPPDs, pions and kaons may be separated up to 10-20 GeV. A precision time-of-flight system would be a valuable resource to the users of the FTBF whose experiments and detector components respond differently based on particle species. The main goals of this stage of experimentation (phase 0) is to build and test a prototype LAPPD TOF system, including design of the fixturing hardware, HV distribution, electronics, synchronization, and triggering configurations for a later iteration: a four-LAPPD time-of-flight system. Long-term goals of the LAPPD TOF project are (1) to design and operate a four-LAPPD TOF system that can be integrated as a permanent particle identification diagnostic for the FTBF and (2) to validate a new commercially available detector technology for detectors in the Energy and Luminosity frontiers.

Setup

The time-of-flight setup is situated on an 80/20 holding-frame behind the MT6.2 pion beam-dump next to the control room. Scintillating paddles and PMTs detect muons that penetrate the pion beam-dump in coincidence with the MTest spill cycle. The PMT signals are discriminated by NIM logic modules to produce a trigger signal for LAPPD front-end electronics. The LAPPDs are mounted inside two dark-boxes with adjustable position (seen in Figure 50). Front-end electronics trigger LAPPD pulses that are recorded in coincidence with muons from beam spills. The PSEC4 ACDC/ACC fast-waveform digitizing electronics are used to digitize 120 channels of LAPPD data at 10.24 GSPS with a buffer depth of 25 ns.

Four boards are synchronized using an arbitrary waveform generator and signal splitters. A rack, NIM crate, HV supplies for PMTs, and Berkeley Cows have been provided by a mixture of the FTBF and Fermilab PREP. PMTs for scintillating paddles were provided by the FTBF. The 80/20 framing was provided by FTBF. Todd Nebel from the FTBF assisted heavily throughout the construction and operation of the setup. Evan Niner, Mandy Rominsky, and Eugene J. Schmidt assisted with hardware, computing, and facility related tasks. A windows computer in the FTBF was used for firmware adjustments of the front-end electronics. Front-end electronics, front-end DAQ computer, and all other instrumentation was provided by U. of C.

Figure 50: Photograph of the setup with two dark-boxes housing two Incom LAPPDs, positioned outside of the enclosure behind the pion beam dump.

Results and Publications

One result of this phase of the experiment was the first iteration design of the hardware described in the setup section. Almost all components of this setup will have upgrades informed by experiences in this phase 0 stage. LAPPDs were integrated into a national lab and beam-line environment for the first time. LAPPDs measured charged particles using Cherenkov light generated in the window for the first time. Multiple LAPPDs were synchronized for the first time. The full photosensitive area of an LAPPD was digitized for the first time using 60 channels of PSEC4 digitizers. Methods were developed for safely and securely holding LAPPDs, communicating to multiple front-end electronics boards, synchronizing boards, using two-sided and single-sided readout geometries, and triggering from a delayed NIM generated beam-signal. Maximum trigger rates and trigger efficiencies were characterized for a two-LAPPD setup with four ACDC boards. Preliminary analyses show undeflected muon-like signals on two simultaneously triggered LAPPDs, example shown in Figure 51. Key improvements for the next phase of experimentation include a White Rabbit picosecond level syncrhonization system, electronics sampling improvements that will improve timing resolution, electronics dead-time reduction, improvements in trigger efficiency, and more robust LAPPD fixturing.

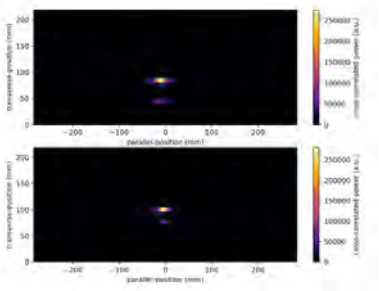

Figure 51: An example of 2-D position reconstruction of a muon-like event on two LAPPDs. The bright spots are an image of many photons on produce in the window of the detector.

21 NOvA

A. Sousa and M. Wallbank, University of Cincinnati, for the NOvA Collaboration

Beam Used: 0.3 2.0 GeV tertiary proton, pions, electrons, muons, kaons; Obtained from MCenter 8-64 GeV secondary protons, pions; Ran at 1.0E8 1.6E10 ppp intensity for primary 120 GeV proton beam.
Run Dates: 05/04/19 06/04/19 Beamline-only, commissioning, one test run with warm APDs in detector. 06/05/19 07/06/19 Beamline + Detector (cooled), commissioning.

Motivation and Goals

The NOvA experiment intends to run until decommissioning of the NuMI beam is required for construction of the Long- Baseline Neutrino Facility in 2025. With this extended running, anticipated increases in the beam intensity and yield, and improvements to the data analysis, NOvA has an opportunity to address many remaining questions in neutrino oscillations, such as the neutrino mass hierarchy, the octant of the atmospheric mixing angle, and the bracketing of the parameter space for leptonic CP violation. A failure to reduce the present level of systematic uncertainties, many of which related to the energy calibration of the detector, could put this opportunity out of reach. The NOvA Test Beam program is aimed at providing tagged electron, muon, pion, and proton beams to enable a detailed understanding of the detector's muon energy scale, and electromagnetic and hadronic response. In addition, Test Beam data will provide real data for the detailed study of particle identification techniques, potentially making essential contributions to the NOvA physics reach, and accelerating NOvA's physics milestones.

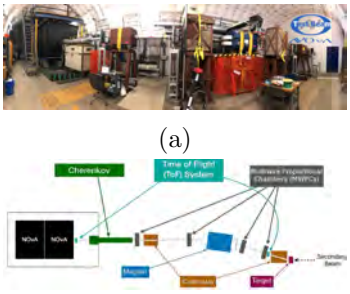

(a)

(b)

Figure 52: The NOvA test beam setup.

Setup

The picture and diagram above show the new tertiary beamline and a scaled-down version of the NOvA detectors, using the same geometry, readout, and electronics as the NOvA Near and Far detectors. Beamline and detector were deployed in the MC7 enclosure, downstream of the Jolly Green Giant magnet, following removal of the MIPP experiment instrumentation that occupied that space, during a period spanning March 2018 to April 2019. A protective firewall was build to insulate the NOvA area from the upstream MC7 areas, given potential fire hazards from liquid scintillator use. A brand new HVAC system was deployed for environment control of the detector electronics and readout, which are particularly sensitive to high humidity, and to regulate scintillator expansion and contraction within the detector. The beamline shares many design characteristics with the MINERvA and LArIAT tertiary beamlines, using the same type of copper target, MWPCs provided by FTBF, and a 16° collimator deflection angle like MINERvA (LArIAT used 13°). Besides the larger TOF lever arm (13.2 m instead of 7 m for LarIAT), the NOvA beamline uses a single refurbished 42 sweeping dipole instead of two large-aperture NDB dipoles. The magnet is interlocked so that the power supplies located in MS5 are turned off when interlocks are broken, but can remain on during a controlled access. Further, a 3 m-long, CO_2-filled, single-PMT Cherenkov counter was deployed to improve electron tagging. A scintillator filling system was deployed in the downstream most part of MC7, using a tanker or totes filled with scintillator placed in a new deployed containment outside MC7. A manually moveable platform allows access to the top of the detector. The racks containing beamline and detector readout, controls, and power supplies are smoke detector-protected, and the detector power supplies are interlocked with environmental controls. Additional shielding was deployed by MC7s North roll-up door, along with additional chipmunk radiation monitors, as part of a complete MC7 radiation assessment carried out by Rad. Safety. The experiment can be fully controlled from the MCenter Control Room, or from an identical setup at ROC-West. Four monitoring cameras have

been installed in MC7, along with a variety of environmental sensors and cosmic and beam rate counters.

Results and Publications

The commissioning data taken so far shows the beamline and filled and instrumented detector block are fully operational. The plot on the right is a preliminary demonstration of the beamlines ability to tag different particle types. Several particles tagged by the beamline were synced with detector activity. Significant primary beam halo activity, appearing to arise from muons, interferes with detector data collection at higher beam intensities. Mitigating measures are being explored and pursued during the summer shutdown. Preparations to fill the second detector block with liquid scintillator are underway. Data-taking operations are expected to resume in Fall 2019 and continue through end of Spring 2020.

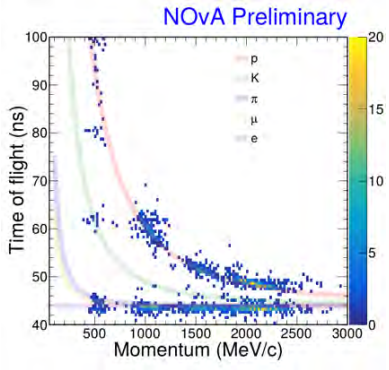

Figure 53: Preliminary TOF vs Momentum plot for various tertiary particles collected during commissioning of the NOvA Test Beam program. The lines show the predictions for each particle.

A Publications

T1429

- B. Azmoun, et al.,"Results From a Prototype Combination TPC Cherenkov Detector With GEM Readout", IEEE Trans. Nucl. Sci. Vol 66, No.8 (2019) 1984-1992.

LArIAT

- G. Pulliam, "π^+ Cross Section on Argon for the LArIAT Experiment.," FERMILAB-THESIS-2019-10.

- W. M. Foreman, "A Demonstration of Light-Augmented Calorimetry For Low-Energy Electrons in Liquid Argon.," FERMILAB-THESIS-2019-01.

- E. Gramellini, "Measurement of the Negative Pion and Positive Kaon Total Hadronic Cross Sections on Argon at the LArIAT Experiment," FERMILAB-THESIS-2018-24.